

A MULTIPHASE MODEL OF TUMOR AND TISSUE GROWTH INCLUDING CELL ADHESION AND PLASTIC REORGANIZATION

LUIGI PREZIOSI* and GUIDO VITALE†

*Dipartimento di Matematica, Politecnico di Torino,
c.so Duca degli Abruzzi 24, Torino 10123, Italy*

**luigi.preziosi@polito.it*

†guido.vitale@polito.it

Received 13 April 2010

Revised 22 October 2010

Communicated by J. T. Oden

The main aim of the paper is to embed the experimental results recently obtained studying the detachment force of single adhesion bonds in a multiphase model developed in the framework of mixture theory. In order to do that the microscopic information is upscaled to the macroscopic level to describe the dependence of some crucial terms appearing in the PDE model on the sub-cellular dynamics involving, for instance, the density of bonds on the membrane, the probability of bond rupture and the rate of bond formation. In fact, adhesion phenomena influence both the interaction forces among the constituents of the mixtures and the constitutive equation for the stress of the cellular components. Studying the former terms a relationship between interaction forces and relative velocity is found. The dynamics presents a behavior resembling the transition from epithelial to mesenchymal cells or from mesenchymal to amoeboid motion, though the chemical cues triggering such transitions are not considered here. The latter terms are dealt with using the concept of evolving natural configurations consisting in decomposing in a multiplicative way the deformation gradient of the cellular constituent distinguishing the contributions due to growth, to cell rearrangement and to elastic deformation. This allows the description of situations in which if in some points the ensemble of cells is subject to a stress above a threshold, then locally some bonds may break and some others may form, giving rise to an internal reorganization of the tissue that allows to relax exceedingly high stresses.

Keywords: Multiphase modeling; cell motion; adhesion.

AMS Subject Classification: 22E46, 53C35, 57S20

1. Introduction

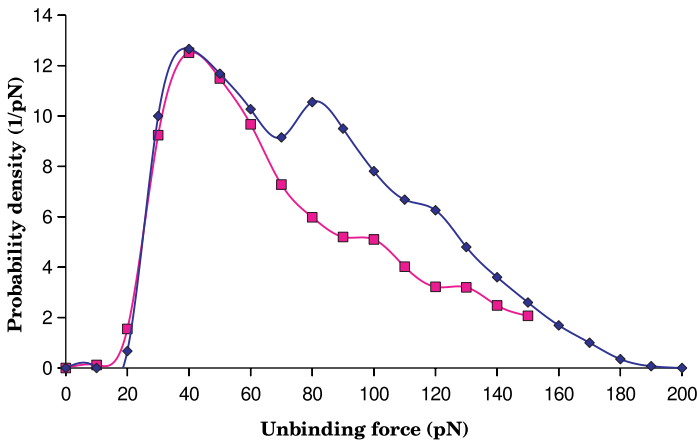
Starting from the paper,²⁰ in the last few years several multiphase models have been developed and applied with success to describe tumor growth. As reviewed in Refs. 3, 7, 16, 30, 39, 52 and 61 most of the models use fluid-like constitutive equations for the cellular constituent. However, this is only an approximation, because tumors and

multicellular spheroids, as most tissues, are more complex, showing solid-like properties associated with the adhesive characteristics of cells. Only recently some attention has been paid to such adhesive interactions between cells and between cells and extracellular matrix (ECM)^{10,11,23,31,40,66} and how these mechanisms influence the behavior of cell aggregates and therefore the detachment of metastases. All the models above, including the one presented here, work at a tissue level, though the experiments studying adhesions are done at a molecular scale. In fact, what is usually measured is the strength of single or clustered adhesion bonds formed by a cell (see, for instance, Refs. 14, 21, 48 and 59). The typical experiment is done using an atomic force microscopy cantilever with a tip that can be possibly functionalized with proper adhesion molecules to check the specific interaction of the cell adhesion molecules with those placed on the tip of the cantilever. After putting the tip in contact with the cell for some time, either the cantilever or the plate with the cell is pulled away at a constant speed, typically in the range $0.2\text{--}5\ \mu\text{m/s}$. If the tip of the cantilever does not attach to the cell, when the cell is moved away, the cantilever does not deflect. This behavior is experimentally obtained, for instance, by the addition of an antibody attaching to the external domain of the adhesion molecule,¹⁴ or by interfering with the links between the adhesion molecules and the cell cytoskeleton,²¹ or by disrupting the actin cytoskeleton.⁵⁹ On the other hand, adhesion gives rise to the deflection of the cantilever that can be related to the stretching force exerted by the cell. Of course, with time the distance between the cell and the cantilever increases, increasing the deflection angle and the stretching force. It is then observed that after some time one or more adhesive bonds break causing a characteristic jump in the deflection of the cantilever that tends to return to its undeformed configuration. In this way it is possible to evaluate the maximum force exerted by an adhesion bond before breaking.

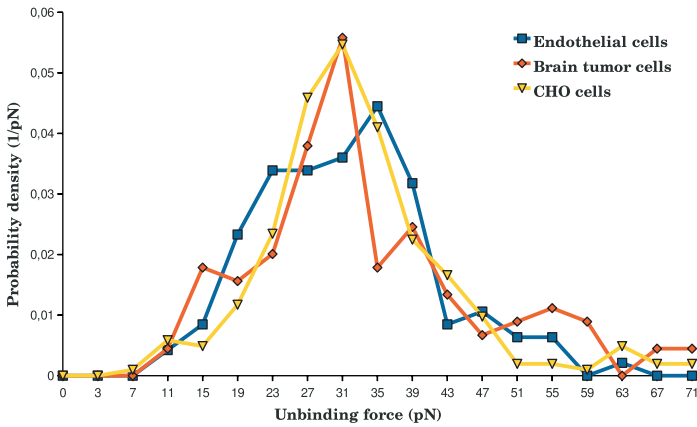
Baumgartner *et al.*¹⁴ found that the mean strength of the adhesion bonds is in the range $35\text{--}55\ \text{pN}$ giving a distribution function of the critical unbinding force like the one shown in Fig. 1(a).

Similar results were obtained by Canetta *et al.*,²¹ and Sun *et al.*⁵⁹ (see Fig. 1(b)). In particular, Sun *et al.*⁵⁹ did not functionalize the microsphere and allowed a longer resting period on the cell surface, ranging from 2 to 30 s. Again, pulling away the cantilever at a constant speed in the range $3\text{--}5\ \mu\text{m/s}$ caused the rupture of one or more adhesive bonds. They used different cell types (Chinese hamster ovary cells CHO, endothelial cells and human brain tumor cells), all showing a mean adhesive strength of a single bond slightly below $30\ \text{pN}$ (see Fig. 1(b)).

Panorchan *et al.*⁴⁸ attach to the cantilever a cadherin-expressing cell, similar to the cell attached to the substratum. The time of contact is short, in order to have the formation of a very limited number of adhesion bonds. The rupture force is found to increase with the loading rate and it is much smaller when N-cadherin bonds are involved (up to $40\ \text{pN}$) rather than E-cadherin bonds (up to $73\ \text{pN}$ for a loading rate of $1000\ \text{pN/s}$ and $157\ \text{pN}$ for a loading rate of $10,000\ \text{pN/s}$).



(a)



(b)

Fig. 1. (Color online) Distribution function of the force of unbinding events (a) when a single bond is acting (red) and when more adhesion bonds are clustering (blue) (data from Ref. 14) and (b) for different types of cells (data from Ref. 59).

In order to utilize these data in a multiphase (PDE) model like the one used in this paper, one needs to upscale the results of the above experiments to the macroscopic scale. Specifically, one needs to describe how the attachment/detachment behavior of the ensemble of adhesion sites linking the cells with the surrounding ECM influences the constitutive equation related to the interaction force between the cellular and the extracellular constituent present in the multiphase model. When describing the behavior of the actin cytoskeleton, Ölz and Schmeiser^{47,46,56} faced a similar problem because they needed to relate the link between the adhesion of the single actin filaments to the behavior of the whole cytoskeleton. Using some of their ideas we here

solve the problem in a multiphase framework. According to the characteristics of the data measured at the microscopic level on the detachment force of single adhesion bonds, which are found to depend on the type of cells, we deduce different relationships for the interaction force, which might correspond to the different migration behaviors of the cell population. First, we distinguish between a Darcy's-like contribution related to the tortuosity and the porosity of the ECM and a contribution due to the adhesion of cells on the ECM. An analytical relation is found relating the terms in the macroscopic model to microscopic quantities like the probability of bond rupture, the density of adhesive molecules on the membrane, the rate of bond formation, the possible continuous renewal of bonds due to spontaneous internalization and externalization, and the strength of the single bonds. The dynamics generated by such laws presents similarities with the transition from epithelial to mesenchymal cells or from mesenchymal to amoeboid motion, and vice versa, though the chemical cues triggering such transitions, which at least as a first approximation influence the just mentioned microscopic parameters, are out of the scope of this paper.

Another term in multiphase models in which adhesion mechanisms among cells play a relevant role is the stress tensor of the cellular constituent. In particular, roughly speaking if the ensemble of cells is subject to a moderate stress everywhere, then the cells and the adhesion bonds will slightly deform but will not break. If instead in some points the ensemble of cells is subject to a sufficiently high stress, then locally some bonds may break and some others may form, giving rise to an internal reorganization of the tissue that allows the relaxation of exceedingly high stresses. In particular, such mechanisms of cell attachment/detachment can be relevant during growth, when duplicating cells displace their neighbors to make room for themselves and eventually for their daughter cells, or when the tumor mass compresses the surrounding tissues. In order to put this observation in a mathematical form, we developed a constitutive model based on the concept of multiple (or evolving) natural configurations introduced by Rajagopal and coworkers and applied to biological tissues in Refs. 12, 32, 33, 42 and 54, and in particular to tumor growth problems in Refs. 1 and 2 (see also Ref. 63 for a review). In Ref. 4 a constitutive model was introduced characterized by the presence of a yield-like condition distinguishing the situation in which the ensemble of cells deforms without undergoing internal reorganization by the one characterized by plastic-like deformations.

In Ref. 50 it was proved that the model proposed in Ref. 4 was able to describe both the shear experiments performed by Jordan *et al.*³⁵ and the compression experiments performed by Forgacs and coworkers.^{25,26,65}

Here, coherently with the concept of load threshold of the adhesion bonds, we merge the above results with the treatment of the attachment between cells and ECM.

The plan of the paper is the following. After this introduction and an introductory section on some aspects related to kinematics, Sec. 3 deals with the interaction force between different constituents for which adhesion plays a relevant role. This in

particular occurs for cells and ECM. In Sec. 4 some examples of macroscopic interaction laws are deduced analytically, starting from available microscopic data and characteristics. The section pays a particular attention to the relationship between the properties of the distribution function of the force giving rise to unbinding events and the properties of the interaction force of the multiphase model. Section 6 describes how to introduce cell–cell adhesion and detachment properties in the constitutive equation for the stress tensor, describing how this is related to the internal reorganization of cells. After presenting some preliminary results in Sec. 5, a final section briefly points out some possible developments.

2. Kinematics

As is well known, tumors and biological tissues in general are made of several mechanically interacting constituents: cells of different type, ECM components, blood, lymphatic vessels, and extracellular liquid. With this in mind, consider two continuum bodies \mathcal{B}^α and \mathcal{B}^β of the mixture and their motion maps χ^α and χ^β defined as

$$\chi^\alpha(\cdot, \tau) : \mathcal{B}^\alpha \rightarrow \mathcal{B}_\tau^\alpha \subset \mathcal{A}, \quad \tau \in [0, T], \tag{2.1}$$

where \mathcal{B}_τ^α is the configuration of the α -body manifold at time τ , embedded in the affine space \mathcal{A} , with tangent bundle $\mathbb{T}\mathcal{A}$. The definition of χ^β is obviously similar. In the same way, in the following when introducing the definition for the constituent α , a similar definition holds also for the constituent β .

In order to avoid confusion between particles belonging to each constituent we refer to material points $X^\alpha \in \mathcal{B}^\alpha$ as α -points, while calling the motion that they undertake α -motion. We consider the mixture manifold as the Cartesian product of the two-body manifold considered $\mathcal{B}^\alpha, \mathcal{B}^\beta$. Any field f defined on such a mixture is a mapping

$$f : (\mathbf{X}^\alpha \in \mathcal{B}^\alpha, \mathbf{X}^\beta \in \mathcal{B}^\beta, t \in [0, T]) \mapsto f(\mathbf{X}^\alpha, \mathbf{X}^\beta, t) \in \text{im}(f).$$

Other descriptions, such as the Eulerian one in the current configuration at the current time t can be obtained straightforwardly using the motions defined in (2.1) (see Refs. 17, 18 and 64).

We define the velocity of a constituent α as

$$\mathbf{v}^\alpha(\mathbf{X}^\alpha, t) := \left(\frac{\partial}{\partial t} \chi^\alpha \right) (\mathbf{X}^\alpha, t) \in \mathbb{T}_{\chi^\alpha(\mathbf{X}^\alpha, t)} \mathcal{A}. \tag{2.2}$$

Another useful quantity that can be defined, provided some regularity of the α -motion, is the α -deformation gradient

$$\mathbf{F}^\alpha(\mathbf{X}^\alpha, t) := \text{Grad}^\alpha \chi^\alpha(\mathbf{X}^\alpha, t) \in \text{Lin}(\mathbb{T}_{\mathbf{X}^\alpha} \mathcal{B}^\alpha, \mathbb{T}_{\chi^\alpha(\mathbf{X}^\alpha, t)} \mathcal{A}), \tag{2.3}$$

indicating with Grad^α the differentiation with respect to \mathbf{X}^α . The tensor \mathbf{F}^α maps the set of all vectors tangent to \mathcal{B}^α in \mathbf{X}^α (say, in $\mathbb{T}_{\mathbf{X}^\alpha} \mathcal{B}^\alpha$) onto $\mathbb{T}_{\chi^\alpha(\mathbf{X}^\alpha, t)} \mathcal{A}$. Since

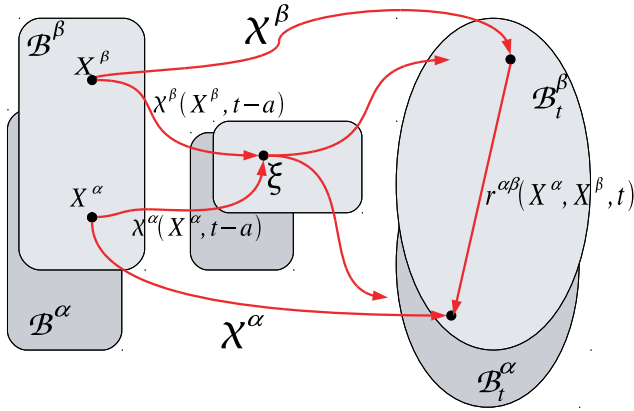


Fig. 2. Superposition of material points of different bodies.

some smoothness is assumed for χ^α , a three-dimensional region of the reference configuration cannot collapse under the α -motion: loosely speaking, no cracks or compenetration are allowed.

We are going to describe a special type of mixture, in which the fields are allowed to depend on the point of the bodies that were superposed somewhere in time, for instance, because of the formation of some adhesive bonds. This mixture is a slight generalization of the one presented in Ref. 49. As sketched in Fig. 2, let then $\chi^\beta(\mathbf{X}^\beta, t - a) = \chi^\alpha(\mathbf{X}^\alpha, t - a) = \xi$, we will state for every field f that

$$f(\mathbf{X}^\alpha, \mathbf{X}^\beta, t) = \tilde{f}(\xi, t). \tag{2.4}$$

It is also useful to introduce the quantity

$$\mathbf{r}^{\alpha\beta}(\mathbf{X}^\alpha, \mathbf{X}^\beta, t) := \chi^\alpha(\mathbf{X}^\alpha, t) - \chi^\beta(\mathbf{X}^\beta, t). \tag{2.5}$$

Referring to Fig. 2, since the body points \mathbf{X}^α and \mathbf{X}^β were superposed at time $t - a$, we remark that

$$\mathbf{X}^\beta = \chi^{\beta-1}(\xi, t - a) = \chi^{\beta-1}(\chi^\alpha(\mathbf{X}^\alpha, t - a), t - a). \tag{2.6}$$

The vector field $\mathbf{r}^{\alpha\beta}$ can then be written as

$$\mathbf{r}^{\alpha\beta}(\mathbf{X}^\alpha, \mathbf{X}^\beta, t) = \chi^\alpha(\mathbf{X}^\alpha, t) - \chi^\beta(\chi^{\beta-1}(\chi^\alpha(\mathbf{X}^\alpha, t - a), t - a), t). \tag{2.7}$$

In this special kind of mixture, discussed in greater detail in the constitutive theory, any field can be described uniquely by prescribing the α -point \mathbf{X}^α and the time lapse a measuring the time passed from the superposition. It means that, instead of a product of two-body manifolds, we can refer to the four-dimensional manifold $\mathcal{B}^\alpha \times [0, t)$. This kind of mixture requires, roughly speaking, an additional scalar coordinate to fully specify a field (in contrast with all previous theories, see Refs. 17–19, 49 and 64). So, by a field f on the mixture, we shall intend the

mapping

$$f : (\mathbf{X}^\alpha \in \mathcal{B}^\alpha, a \in [0, t], t \in [0, T]) \mapsto f(\mathbf{X}^\alpha, a, t) \in \text{im}(f). \tag{2.8}$$

We point out that the material derivative, using this type of description, is well defined as

$$\begin{aligned} \dot{f}(\mathbf{X}^\alpha, a, t) &:= \lim_{h \rightarrow 0} \frac{f(\mathbf{X}^\alpha, a + h, t + h) - f(\mathbf{X}^\alpha, a, t)}{h} \\ &\equiv \frac{\partial f}{\partial t}(\mathbf{X}^\alpha, a, t) + \frac{\partial f}{\partial a}(\mathbf{X}^\alpha, a, t), \end{aligned} \tag{2.9}$$

which holds constant the time of superposition $t - a$. For fields declared to be independent from a : $\dot{f}(\mathbf{X}^\alpha, t) \equiv \frac{\partial}{\partial t} f(\mathbf{X}^\alpha, t)$.

It is interesting for future developments to compare here the typical age of a bond A with the characteristic time T related to cell motion, which can be related to the cell size L and the characteristic velocity of cell motion V through $T = L/V$. T is then the time needed by a cell to move across a cell length that using physiological values is at least of the order of few minutes. On the other hand, due to the fast trafficking of adhesion molecules coming back and forth from the membrane A is of the order of few seconds (see, for instance, Refs. 14, 62 and 67). This behavior, which from the biological viewpoint is understood to lead to cell plasticity, from the mathematical viewpoint leads to the existence of a small parameter $\epsilon = A/T$, which allows one to study the limit $\epsilon \ll 1$ that in dimensional terms corresponds to what we will denote with the dimensional limit $a \rightarrow 0$.

Defining $\mathbf{x} := \chi^\alpha(\mathbf{X}^\alpha, t)$, for small a one has

$$\chi^\alpha(\mathbf{X}^\alpha, t - a) \simeq \mathbf{x} - a \frac{\partial}{\partial t} \chi^\alpha(\mathbf{X}^\alpha, t), \quad a \rightarrow 0. \tag{2.10}$$

Next we consider

$$\begin{aligned} &\chi^{\beta-1} \left(\mathbf{x} - a \frac{\partial}{\partial t} \chi^\alpha(\mathbf{X}^\alpha, t), t - a \right) \\ &\simeq \chi^{\beta-1}(\mathbf{x}, t) - a \frac{\partial}{\partial t} (\chi^{\beta-1})(\mathbf{x}, t) - a \text{grad}(\chi^{\beta-1})(\mathbf{x}, t) [\mathbf{v}^\alpha(\mathbf{X}^\alpha, t)] \\ &= \chi^{\beta-1}(\mathbf{x}, t) + a \mathbf{F}^{\beta-1}(\mathbf{x}, t) [\mathbf{v}^\beta(\chi^{\beta-1}(\mathbf{x}, t), t)] \\ &\quad - a \mathbf{F}^{\beta-1}(\mathbf{x}, t) [\mathbf{v}^\alpha(\mathbf{X}^\alpha, t)], \quad a \rightarrow 0, \end{aligned} \tag{2.11}$$

where grad means the differentiation with respect to the first argument of $\chi^{\beta-1}$ (i.e. \mathbf{x}) and we used the facts that

$$\frac{\partial}{\partial t} \chi^{\beta-1}(\mathbf{x}, t) = -\mathbf{F}^{\beta-1} [\mathbf{v}^\beta(\chi^{\beta-1}(\mathbf{x}, t), t)], \tag{2.12}$$

and

$$\text{grad} \chi^{\beta-1}(\mathbf{x}, t) = \mathbf{F}^{\beta-1}(\mathbf{x}, t). \tag{2.13}$$

Using (2.10) and (2.11), we can approximate (2.7) as

$$\begin{aligned} \mathbf{r}^{\alpha\beta} &\simeq \mathbf{x} - \chi^\beta \left(\chi^{\beta-1}(\mathbf{x}, t) + a \mathbf{F}^{\beta-1}(\mathbf{x}, t) \frac{\partial}{\partial \tau} \chi^\beta(\chi^{\beta-1}(\mathbf{x}, t), \tau) \Big|_{\tau=t} \right. \\ &\quad \left. - a \mathbf{F}^{\beta-1}(\mathbf{x}, t) \frac{\partial}{\partial t} \chi^\alpha(\mathbf{X}^\alpha, t), t \right) \\ &\simeq -a \text{Grad} \chi^\beta(\chi^{\beta-1}(\mathbf{x}, t), t) \left\{ \mathbf{F}^{\beta-1}(\mathbf{x}, t) + \left[\frac{\partial}{\partial \tau} \chi^\beta(\chi^{\beta-1}(\mathbf{x}, t), \tau) \Big|_{\tau=t} \right. \right. \\ &\quad \left. \left. - \frac{\partial}{\partial t} \chi^\alpha(\mathbf{X}^\alpha, t) \right] \right\}, \quad a \rightarrow 0, \end{aligned}$$

and, since $\text{Grad} \chi^\beta(\chi^{\beta-1}(\mathbf{x}, t), t) = \mathbf{F}^\beta(\mathbf{x}, t)$

$$\begin{aligned} \mathbf{r}^{\alpha\beta}(\mathbf{x}, t) &\simeq -a \left[\frac{\partial}{\partial \tau} \chi^\beta(\chi^{\beta-1}(\mathbf{x}, t), \tau) \Big|_{\tau=t} - \frac{\partial}{\partial t} \chi^\alpha(\mathbf{X}^\alpha, t) \right] \\ &\simeq a(\mathbf{v}^\alpha(\mathbf{x}, t) - \mathbf{v}^\beta(\mathbf{x}, t)), \quad a \rightarrow 0, \end{aligned} \tag{2.14}$$

where the Eulerian description of velocities is used. In other words, (2.14) means

$$\frac{\partial \mathbf{r}^{\alpha\beta}}{\partial a}(\mathbf{x}, 0, t) = \mathbf{v}^\alpha(\mathbf{x}, t) - \mathbf{v}^\beta(\mathbf{x}, t). \tag{2.15}$$

3. Interaction Force between Constituents

Referring to Refs. 3 and 30 for more details, the general structure of multiphase models consists in a set of mass and momentum balance equations for the constituents. The former can be written as

$$\frac{\partial \phi_\alpha}{\partial t} + \text{div}(\phi_\alpha \mathbf{v}_\alpha) = \Gamma_\alpha, \tag{3.1}$$

where ϕ_α is the volume ratio of the constituent, and Γ_α is its growth/death term. On the other hand, considering that inertia is negligible in the description of growth phenomena, the latter can be written as

$$\text{div}(\phi_\alpha \mathbf{T}_\alpha) + \mathbf{m}_\alpha = \mathbf{0}, \tag{3.2}$$

where \mathbf{T}_α is the Cauchy partial stress tensor, and \mathbf{m}_α is the interaction force, also named momentum supply. In this section we will focus on this last term. Having neglected inertia, the contribution of the momentum supply given by mass exchange can be neglected as well.⁵¹ This means that \mathbf{m}_α only measures the forces acting on the α -constituent due to its interactions with the other constituents of the mixture. The interaction force then is intrinsically defined on the whole mixture manifold, while other quantities, like stress tensors and densities, are defined only on the single body and no meaningful extension exists out of this manifold. Also balance equations are defined on the body *per se* but the presence of interaction forces constitutes a link among the bodies.

The general model that can be rather complicated was simplified in Ref. 53 to more manageable models under two basic assumptions: the first one consists in assuming that the components of the ECM and possibly of the vasculature form such an intricate network that they all move together so that the same deformation and velocity describe their evolution (actually, in many cases the ECM is assumed to be rigid). The second one consists in the observation that the interaction forces between the liquid and the other constituents are of the same order as the pressure gradient and much smaller than, for instance, the internal stresses of the solid constituents or the adhesion forces acting between cells and ECM. This allows one to simplify (3.2) as

$$\sum_{\beta} \mathbf{m}^{\alpha\beta} = -\operatorname{div}(\phi_{\alpha} \mathbf{T}'_{\alpha}), \tag{3.3}$$

where in the summation the contribution due to the interaction with the liquid is missing and \mathbf{T}'_{α} is the excess stress tensor.

For sake of clarity, the reader may think of the indices α and β as those referring, respectively, to the cell population and to the ECM, though the argument has a wider generality and can be, for instance, applied to cells of different type. When dealing with cell–ECM interactions, we distinguish in $\mathbf{m}^{\alpha\beta}$ two types of contributions: the former is related to the tortuosity of the ECM and therefore to the fact that the cells have to move in an intricate network of fibers. Hence, even in absence of adhesive interactions the ensemble of cells moves in a porous-like medium so that the interaction force can be modeled by the classical term leading to Darcy’s law

$$\mathbf{m}_D^{\alpha\beta}(\mathbf{x}, t) = -M(\mathbf{v}^{\alpha}(\mathbf{x}, t) - \mathbf{v}^{\beta}(\mathbf{x}, t)), \tag{3.4}$$

where the spatial description of the fields is used, since Darcy’s law is a local type interaction between points superposed in the current configuration. The latter is related to the adhesion between the constituents. Therefore, even if cells were in a straight channel in the ECM and the force were aligned to it, the ensemble of cells would still experience a traction force $\mathbf{m}_{\text{ad}}^{\alpha\beta}$ due to the adhesive interaction with the ECM.

Entering into more detail, we call the *microscopic force* the force $\mathbf{F}_{\text{mic}}^{\alpha}(\mathbf{X}^{\alpha}, \mathbf{X}^{\beta}, t)$ acting on $\mathbf{X}^{\alpha} \in \mathcal{B}^{\alpha}$ because of the adhesive interaction with $\mathbf{X}^{\beta} \in \mathcal{B}^{\beta}$. The total momentum exchanged in \mathbf{X}^{α} with the manifold \mathcal{B}^{β} due to adhesion forces is

$$\mathbf{m}_{\text{ad}}^{\alpha\beta}(\mathbf{X}^{\alpha}, t) := \int_{\mathcal{B}^{\beta}} \mathbf{F}_{\text{mic}}^{\alpha\beta}(\mathbf{X}^{\alpha}, \mathbf{Y}, t) d\mathbf{Y} \in \mathbb{T}_{\chi^{\alpha}(\mathbf{X}^{\alpha}, t)}^* \mathcal{A}. \tag{3.5}$$

Using the hypothesis in (2.4) we have the nice formula

$$\mathbf{m}_{\text{ad}}^{\alpha\beta}(\mathbf{X}^{\alpha}, t) = \int_0^{+\infty} \mathbf{F}_{\text{mic}}^{\alpha\beta}(\mathbf{X}^{\alpha}, a, t) \mu(da). \tag{3.6}$$

We point out that, for us, the measure $\mu(da)$ or $d\mathbf{Y}$ are to be *a priori* given. An example will be exploited in the following section.

It is worth stating a balance equation for the momentum exchange term that reflects the fact that we want Newton's second law satisfied even in the mixture manifold and not only on the single bodies ($\mathbf{m}^{\alpha\beta}$ is external for a body and internal for the mixture as a whole). The simplest law we are able to think of is (see Ref. 49)

$$\mathbf{F}_{\text{mic}}^{\alpha\beta}(\mathbf{X}^\alpha, \mathbf{X}^\beta, t) + \mathbf{F}_{\text{mic}}^{\beta\alpha}(\mathbf{X}^\beta, \mathbf{X}^\alpha, t) = 0, \quad \forall \mathbf{X}^\alpha \in \mathcal{B}^\alpha, \mathbf{X}^\beta \in \mathcal{B}^\beta. \quad (3.7)$$

We take as *basic fields* only the motions χ^α, χ^β as defined in (2.1) since we want to keep the discussion at a minimum level of complexity. Then, to take adhesion into account, we introduce the scalar internal variable $f^{\alpha\beta}(\mathbf{X}^\alpha, \mathbf{X}^\beta, t)$ related to the probability of forming an adhesion bond between \mathbf{X}^α and \mathbf{X}^β .

Using the field hypothesis (2.4) we can write $f^{\alpha\beta} \equiv f^{\alpha\beta}(\mathbf{X}^\alpha, a, t)$, where a is called *age of the bond*, so that the number density of bonds formed at time t is

$$N^{\alpha\beta}(\mathbf{X}^\alpha, t) = \int_0^{+\infty} f^{\alpha\beta}(\mathbf{X}^\alpha, a, t) da. \quad (3.8)$$

This internal variable has its own balance equation suggested by population dynamics theory³⁴ or kinetic theory¹⁵

$$\dot{f}^{\alpha\beta} := \frac{\partial f^{\alpha\beta}}{\partial t} + \frac{\partial f^{\alpha\beta}}{\partial a} = -\eta^{\alpha\beta}, \quad (3.9)$$

where $\eta^{\alpha\beta}$ has the role of describing detachment processes.

The internal variable $f^{\alpha\beta}$ is also used to specify the measure $\mu(da)$ that is taken to be absolutely continuous and proportional to the bond density $\mu(da) = f^{\alpha\beta}(\mathbf{X}^\alpha, a, t) da$.

We now discuss the constitutive maps for the microscopic force $\mathbf{F}_{\text{mic}}^{\alpha\beta}$ and the detachment rate $\eta^{\alpha\beta}$ while constitutive maps for the stress tensor \mathbf{T}'_α will be discussed in Sec. 5. A *constitutive field* $c \equiv c(\mathbf{X}^\alpha, \mathbf{X}^\beta, t)$ will be here provided with a *constitutive mapping* \hat{c} such that

$$c(\mathbf{X}^\alpha, \mathbf{X}^\beta, t) = \hat{c}(\chi^\alpha, \chi^\beta), \quad (3.10)$$

where for sake of simplicity we consider the homogeneous situation.

Following Ref. 49 we assume that the microscopic force depends on the position, age of the bonds, and time through $\mathbf{r}^{\alpha\beta}$, i.e.

$$\mathbf{F}_{\text{mic}}^{\alpha\beta}(\mathbf{X}^\alpha, a, t) = \widehat{\mathbf{F}}_{\text{mic}}^{\alpha\beta}(\mathbf{r}^{\alpha\beta}(\mathbf{X}^\alpha, a, t)). \quad (3.11)$$

The constitutive relation for $\eta^{\alpha\beta}$ follows from the physical intuition that a bond breaks up depending on the magnitude of the microscopic force exerted on it and on its age

$$\eta^{\alpha\beta}(\mathbf{X}^\alpha, a, t) = \hat{\eta}^{\alpha\beta}(F_{\text{mic}}^{\alpha\beta}(\mathbf{X}^\alpha, a, t), f^{\alpha\beta}(a, t), a), \quad (3.12)$$

where $F_{\text{mic}}^{\alpha\beta} = |\mathbf{F}_{\text{mic}}^{\alpha\beta}|$. Actually, it is also reasonable to assume a linear relationship with $f^{\alpha\beta}$, so that

$$\begin{aligned} \eta^{\alpha\beta}(\mathbf{X}^\alpha, a, t) &= \zeta^{\alpha\beta}(F_{\text{mic}}^{\alpha\beta}(\mathbf{X}^\alpha, a, t), a)f^{\alpha\beta}(a, t) \\ &= \zeta^{\alpha\beta}(\widehat{F}_{\text{mic}}^{\alpha\beta}(\mathbf{r}^{\alpha\beta}(\mathbf{X}^\alpha, a, t)), a)f(a, t). \end{aligned} \tag{3.13}$$

In the next section we will explain how to deduce $\zeta^{\alpha\beta}$ from some experimental data.

As an example we can state a simple linear isotropic map

$$\mathbf{F}_{\text{mic}}^{\alpha\beta}(\mathbf{X}^\alpha, a, t) = -k_{\text{mic}}^{\alpha\beta}\mathbf{r}^{\alpha\beta}(\mathbf{X}^\alpha, a, t), \tag{3.14}$$

where $k_{\text{mic}}^{\alpha\beta}$ is the elastic constant of the microscopic bond. From (3.6) we have

$$\mathbf{m}_{\text{ad}}^{\alpha\beta}(\mathbf{X}^\alpha, t) = -k_{\text{mic}}^{\alpha\beta} \int_0^{+\infty} \mathbf{r}^{\alpha\beta}(\mathbf{X}^\alpha, a, t)f^{\alpha\beta}(\mathbf{X}^\alpha, a, t) da. \tag{3.15}$$

To compare with previous mixture theories, for a moment we leave aside the population dynamics subtleties and rule out an example giving us Darcy’s law, as written in (3.4). To find this famous constitutive map, it is sufficient to set $\mu(da) = C_1\delta_{a=0} - C_2\delta'_{a=0}$,^a and the other maps as before. Referring to (2.14), what can be found is

$$\begin{aligned} \mathbf{m}_{\text{ad}}^{\alpha\beta}(\mathbf{x}, t) &= -k_{\text{mic}}^{\alpha\beta} \int_0^{+\infty} \mathbf{r}^{\alpha\beta}(\mathbf{X}^\alpha, a, t)\mu(da) \\ &= -k_{\text{mic}}^{\alpha\beta} C_2 \frac{\partial \mathbf{r}^{\alpha\beta}}{\partial a}(\mathbf{X}^\alpha, 0, t) \\ &= -k_{\text{mic}}^{\alpha\beta} C_2(\mathbf{v}^\alpha(\mathbf{x}, t) - \mathbf{v}^\beta(\mathbf{x}, t)), \end{aligned} \tag{3.16}$$

where $1/k_{\text{mic}}^{\alpha\beta}$ assumes the meaning of a permeability.

Notice that, from (2.7) and (2.4), $\mathbf{r}^{\alpha\beta}(\mathbf{X}^\alpha, 0, t) = 0$. This type of measure $\mu(da)$ reflects the fact that only the first-order neighborhood with respect to the current configuration $\mathbf{x} = \chi^\alpha(\mathbf{X}^\alpha, t)$ is relevant for momentum exchange.

4. The Quasi-Stationary Limit

The aim of this section is to relate the microscopic measurement with the macroscopic constitutive laws defining the interaction force $\mathbf{m}_{\text{ad}}^{\alpha\beta}$. To simplify the notation we drop in this section the index $\alpha\beta$. A way to upscale the information obtained at the sub-cellular level is suggested by Ölz and Schmeiser who solved in Refs. 46, 47 and 56 a similar problem when dealing with the actin cytoskeleton.

To do that, we need first to join Eq. (3.9) with a proper boundary condition. We could take the rate of bond formation to be constant, but as will be shown at the end of the section, this would give rise in some cases to unreasonable results. A better boundary condition should take into account the fact that the cell can expose on the

^aThe distribution $\delta_{a=0}$ is defined for all continuous field $f: a \in [0, T] \mapsto f(a)$ in such a way that $\delta_{a=0}[f] = f(0)$; similarly $\delta'_{a=0}[f] = -f'(0)$.

membrane a maximum number of adhesion bonds, so that the number density N_{\max} of active bonds per unit volume is in a first approximation proportional to the volume ratio occupied by the cells, or better to the ratio of cell contact area per unit volume. We can then assume that the formation of new bonds is proportional to the bonds that can still be formed, i.e. recalling (3.8),

$$f(a = 0, t) = \beta(N_{\max} - N^{\alpha\beta}(t)) = \beta\left(N_{\max} - \int_0^{+\infty} f(a, t) da\right). \tag{4.1}$$

Using the scaling introduced in Sec. 2, we can rewrite in dimensionless form the problem constituted by (3.9), with η given by (3.13), and (4.1) as

$$\begin{cases} \epsilon \frac{\partial \tilde{f}}{\partial \tilde{t}} + \frac{\partial \tilde{f}}{\partial \tilde{a}} = -\tilde{\zeta}(\tilde{F}_{\text{mic}})\tilde{f}, \\ \tilde{f}(\tilde{a} = 0, \tilde{t}) = \tilde{\beta}\left(1 - \int_0^{+\infty} \tilde{f}(\tilde{a}, \tilde{t}) d\tilde{a}\right), \end{cases} \tag{4.2}$$

where f is scaled with N_{\max}/A , $\tilde{\zeta} = A\zeta$ and $\tilde{\beta} = A\beta$.

In the limit $\epsilon \rightarrow 0$ the problem reduces to its quasi-stationary version, dropping the time derivative in the differential equation and with time taking then the role of a parameter in the boundary condition.

As we prefer to work with dimensional variables, we go back to the dimensional quasi-stationary problem that writes

$$\begin{cases} \frac{\partial f}{\partial a}(a; t) = -\zeta(F_{\text{mic}}(a; t))f(a; t), \\ f(a = 0; t) = \beta\left(N_{\max} - \int_0^{+\infty} f(a; t) da\right). \end{cases} \tag{4.3}$$

For any ζ , the differential equation in (4.3) can be solved giving

$$f(a; t) = C(t) \exp\left[-\int_0^a \zeta(F_{\text{mic}}(\alpha, t)) d\alpha\right], \tag{4.4}$$

where $C(t)$ can be determined through the boundary condition obtaining

$$C(t) = \frac{\beta N_{\max}}{1 + \beta \int_0^{+\infty} \exp\left[-\int_0^{\tilde{a}} \zeta(F_{\text{mic}}(\alpha, t)) d\alpha\right] d\tilde{a}}. \tag{4.5}$$

Hence, dropping the dependence on t , for sake of simplicity,

$$f(a) = \frac{\beta N_{\max} \exp\left[-\int_0^a \zeta(F_{\text{mic}}(\alpha)) d\alpha\right]}{1 + \beta \int_0^{+\infty} \exp\left[-\int_0^{\tilde{a}} \zeta(F_{\text{mic}}(\alpha)) d\alpha\right] d\tilde{a}}, \tag{4.6}$$

and, from (3.6),

$$\mathbf{m}_{ad}^{\alpha\beta} = \frac{\beta N_{max} \int_0^{+\infty} \mathbf{F}_{mic}(a) \exp\left[-\int_0^a \zeta(F_{mic}(\alpha)) d\alpha\right] da}{1 + \beta \int_0^{+\infty} \exp\left[-\int_0^a \zeta(F_{mic}(\alpha)) d\alpha\right] da}. \tag{4.7}$$

If we take $\mathbf{F}_{mic} = -k_{mic} \mathbf{r}^{\alpha\beta}$, by an argument similar to the one above, it can be shown that in the limit $A \ll T$, (i.e. $\epsilon \rightarrow 0$)

$$\mathbf{F}_{mic} = k_{mic} a(\mathbf{v}^\beta - \mathbf{v}^\alpha),$$

and therefore

$$\mathbf{m}_{ad}^{\alpha\beta} = k_{mic} \beta N_{max} (\mathbf{v}^\beta - \mathbf{v}^\alpha) \frac{\int_0^{+\infty} a \exp\left[-\int_0^a \zeta(k_{mic} v_{rel} \alpha) d\alpha\right] da}{1 + \beta \int_0^{+\infty} \exp\left[-\int_0^a \zeta(k_{mic} v_{rel} \alpha) d\alpha\right] da}, \tag{4.8}$$

where $v_{rel} = |\mathbf{v}^\beta - \mathbf{v}^\alpha|$. Referring to the modulus of the microscopic force rather than the age of the bond, we can then write

$$|\mathbf{m}_{ad}^{\alpha\beta}| = \frac{N_{max} \int_0^{+\infty} F e(F) dF}{W + \int_0^{+\infty} e(F) dF}, \tag{4.9}$$

where $W = k_{mic} v_{rel} / \beta$ and

$$e(F) = \exp\left[-\frac{1}{k_{mic} v_{rel}} \int_0^F \zeta(\phi) d\phi\right]. \tag{4.10}$$

Equations (4.8) or (4.9) represent the general dependence of the macroscopic interaction force from the microscopic characteristics of the adhesion bonds, in particular, from the density of bonds on the membrane, the contact area between cells and ECM per unit volume, the rate of bond formation, the bond rigidity, and the detachment rate. In this respect, it can be regarded as a multiscale link between models operating at different scales.

Example 1. If there is a continuous constant renewal of bonds, i.e. $\zeta = \zeta_0$ constant, then

$$f(a) = \frac{\beta \zeta_0 N_{max}}{\beta + \zeta_0} e^{-\zeta_0 a}, \tag{4.11}$$

and

$$\mathbf{m}_{ad}^{\alpha\beta} = -k_{mic} \frac{\beta N_{max}}{\zeta_0(\beta + \zeta_0)} (\mathbf{v}^\alpha - \mathbf{v}^\beta). \tag{4.12}$$

One then finds the classical drag law asserting that in addition to $\mathbf{m}_D^{\alpha\beta}$ also the adhesive interaction force is proportional to the relative velocity, i.e. a Darcy’s-like relationship. So, it does not add any new effect to $\mathbf{m}_D^{\alpha\beta}$ and the two terms can merge in a single one.

Example 2. If the bonds start breaking only after the microscopic force F_{mic} overcomes a threshold F_0 , and is then constant, i.e.

$$\zeta(F_{\text{mic}}) = \zeta_0 H(F_{\text{mic}} - F_0), \tag{4.13}$$

where H is the Heaviside function, then

$$\frac{|\mathbf{m}_{\text{ad}}^{\alpha\beta}|}{N_{\text{max}}} = \frac{\hat{F}_0^2 + \hat{F}_0 F_0 + \frac{1}{2} F_0^2}{W + \hat{F}_0 + F_0}, \tag{4.14}$$

where

$$\hat{F}_0 = \frac{k_{\text{mic}} v_{\text{rel}}}{\zeta_0}. \tag{4.15}$$

For small velocities $|\mathbf{m}_{\text{ad}}^{\alpha\beta}|$ tends to $F_0 N_{\text{max}}/2$ while for large velocities it goes back to the modulus of (4.12) that if the rates of bond formation and association are equal, as plausible, simplify to $k_{\text{mic}} N_{\text{max}} v_{\text{rel}}/(2\beta)$. This behavior, shown in Fig. 3(a), is compatible with the one proposed in Ref. 53 where it is argued that if cells are not pulled strong enough, they move together with the ECM. If the force overcomes the threshold $F_0 N_{\text{max}}/2$, they detach from the ECM.

In spite of the simplicity of (4.12) and (4.14), however, it is more proper to obtain ζ from assumptions or experimental data on the bond-breaking distribution $b(F_{\text{mic}})$ (e.g. those in Fig. 1). In order to do that we distinguish in ζ two contributions: One,

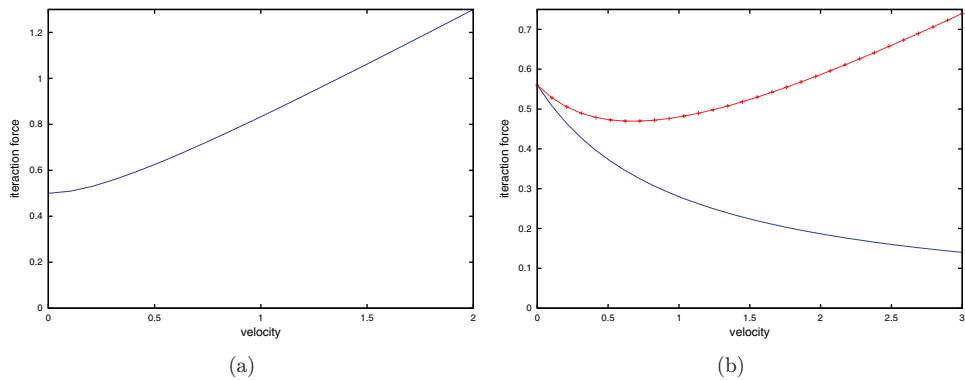


Fig. 3. Macroscopic adhesion laws for different cell–ECM microscopic interaction laws. In (a) $|\mathbf{m}_{\text{ad}}^{\alpha\beta}|/N_{\text{max}}F_0$ versus W/F_0 as given by Eq. (4.14) (Example 2). In (b), referring to the CHO cells data in Ref. 59, $|\mathbf{m}_{\text{ad}}^{\alpha\beta}|/N_{\text{max}}m_b$ (bottom) and $|\mathbf{m}^{\alpha\beta}|/N_{\text{max}}m_b$ (top) related to Example 3 and Eq. (4.24) are plotted versus W/m_b when $M/m_b = 0.2$.

similar to the ones in the two examples above, related to the internal renewal of adhesion molecules, the other (ζ_r) related to the force-induced detachment, e.g.

$$\zeta(F_{\text{mic}}(a)) = \zeta_0 H(F_{\text{mic}}(a) - F_0) + \zeta_r(F_{\text{mic}}(a)). \tag{4.16}$$

This last contribution is related to the breaking distribution b by

$$\zeta_r(F_{\text{mic}}(a)) = \frac{b(F_{\text{mic}}(a))}{B(F_{\text{mic}}(a))} = -\frac{1}{B(F_{\text{mic}}(a))} \frac{dB}{da}(F_{\text{mic}}(a)), \tag{4.17}$$

or, because of the linear dependence of F_{mic} from a ,

$$\zeta_r(F_{\text{mic}}) = -\frac{k_{\text{mic}} v_{\text{rel}}}{B(F_{\text{mic}})} \frac{dB}{dF_{\text{mic}}}(F_{\text{mic}}), \quad \text{for } F_{\text{mic}} < F_M, \tag{4.18}$$

where F_M is the supremum of the support of b , that is compact, and

$$B(F_{\text{mic}}) = \int_{F_{\text{mic}}}^{F_M} b(\phi) d\phi, \tag{4.19}$$

is the survival function. Of course, different breaking distributions would give rise to different macroscopic forces. However, we can state some general properties that can easily be proved.

Property 1. (on B) Since the function $b(F)$ is positive with compact support in $[F_m, F_M]$, then $B(F)$ is constant for $F < F_m$, decreases in (F_m, F_M) , vanishes at $F = F_M$, and has an inflection point corresponding to the maximum of $b(F)$. In addition,

$$\text{if for } F \simeq F_M, \quad b(F) \simeq C_M (F_M - F)^{\alpha_M} \Rightarrow B(F) \simeq \frac{C_M}{\alpha_M + 1} (F_M - F)^{\alpha_M + 1}.$$

Integration by parts gives that the mean value of $b(F)$ is

$$m_b = F_m + \int_{F_m}^{F_M} \frac{B(F)}{B(F_m)} dF, \tag{4.20}$$

and the standard deviation σ is given by

$$\sigma^2 = F_m^2 + 2 \int_{F_m}^{F_M} F \frac{B(F)}{B(F_m)} dF - m_b^2. \tag{4.21}$$

From the data by Baumgartner *et al.*,¹⁴ Panorchan *et al.*⁴⁸ and Sun *et al.*⁵⁹ reported in Fig. 1, we can argue that F_m is about 10 pN, with a slightly larger value in Ref. 48 and a lower value (approximately 4 pN) for the Chinese hamster ovary cells used in Ref. 59. Regarding F_M from the graphs in Ref. 14 it is clear that it is about 200 pN and for the endothelial cells in Ref. 59 it is about 70 pN. The other graphs reported there and in Ref. 48 do not reach zero, so it is hard to evaluate F_M .

Property 2 (on ζ_r). The above property on B implies that the function $\zeta_r(F)$ vanishes for $F \leq F_m$ and blows up at F_M and is not integrable there.

Therefore, for $F \in [F_m, F_M]$,

$$\int_0^F \zeta_r(\phi) d\phi = \int_{F_m}^F \zeta_r(\phi) d\phi = -k_{\text{mic}} v_{\text{rel}} \ln \frac{B(F)}{B(F_m)}. \tag{4.22}$$

Example 3. If $\zeta = \zeta_r$, corresponding to neglecting the continuous renewal of bonds which, for instance, may characterize epithelial cells, we have the strong simplification

$$e(F) = \frac{B(F)}{B(F_m)}. \tag{4.23}$$

Obviously, $e(F) = 1$ for $F < F_m$, and $e(F_M) = 0$. We can then extend $e(F)$ and $B(F)$ assuming that they vanish for $F > F_M$. Hence, from (4.9), (4.20), and (4.21),

$$\frac{|\mathbf{m}_{\text{ad}}^{\alpha\beta}|}{N_{\text{max}}} = \frac{\frac{F_m^2}{2} + \int_{F_m}^{F_M} F \frac{B(F)}{B(F_m)} dF}{W + F_m + \int_{F_m}^{F_M} \frac{B(F)}{B(F_m)} dF} = \frac{\sigma^2 + m_b^2}{2(W + m_b)}, \tag{4.24}$$

which decreases from $b_0 = (1 + \frac{\sigma^2}{m_b^2}) \frac{m_b}{2}$ to zero as the relative velocity increases. This is due to the fact that the high velocity breaks more bonds than the ones that are formed at a rate β . There is, however, a threshold stress determining cell detachment. We remark that m_b and σ are properties of the bond-breaking distribution function that are usually measured. For instance, in Ref. 59 $m_b = 28, 29, 29$ pN and $\sigma = 10, 9, 10$ pN, respectively, for Chinese hamster ovary cells, a malignant human brain tumor cell line, and human endothelial cells (EA hy926). Higher values can be deduced from the data in Ref. 14, which gives $m_b \approx 73$ pN and $\sigma \approx 38$ pN.

Referring to Fig. 3(b), it should be noticed that when $\mathbf{m}_{\text{ad}}^{\alpha\beta}$ and $\mathbf{m}_D^{\alpha\beta}$ are added to get

$$\mathbf{m}^{\alpha\beta} = -N_{\text{max}} \frac{\sigma^2 + m_b^2}{2(W + m_b)} \frac{\mathbf{v}^\alpha - \mathbf{v}^\beta}{v_{\text{rel}}} - M(\mathbf{v}^\alpha - \mathbf{v}^\beta), \tag{4.25}$$

which might have a minimum for

$$v_{\text{rel}} = \sqrt{\frac{(\sigma^2 + m_b^2)\beta}{2k_{\text{mic}}M}} - \frac{\beta m_b}{k_{\text{mic}}}, \quad \text{if } \frac{2\beta M}{k_{\text{mic}}N_{\text{max}}} < 1 + \frac{\sigma^2}{m_b^2}.$$

After that $|\mathbf{m}^{\alpha\beta}|$ grows to infinity because $|\mathbf{m}_D^{\alpha\beta}|$ becomes dominant (otherwise it is always increasing). In this case, starting from rest, when the interaction force overcomes the threshold value b_0 , cells detach to crawl with a velocity given by the right branch, which we will denote Darcy-dominated branch. If now the interaction force decreases below the minimum, then the cells attach again, giving rise to a behavior that is characteristic of bistable systems.

We now consider that in addition to a force-driven detachment, there is a continuous renewal of the bonds. We will assume there this is triggered when $F > F_0$ and

use (4.16). We then have

$$e(F) = \frac{B(F)}{B(F_m)} \exp\left[-\frac{(F - F_0)_+}{\hat{F}_0}\right], \tag{4.26}$$

where h_+ stands for the positive part of h , and

$$\frac{|\mathbf{m}_{ad}^{\alpha\beta}|}{N_{max}} = \frac{\int_0^{F_m} F \exp\left[-\frac{(F-F_0)_+}{\hat{F}_0}\right] dF + \int_{F_m}^{F_M} F \exp\left[-\frac{(F-F_0)_+}{\hat{F}_0}\right] \frac{B(F)}{B(F_m)} dF}{W + \int_0^{F_m} \exp\left[-\frac{(F-F_0)_+}{\hat{F}_0}\right] dF + \int_{F_m}^{F_M} \exp\left[-\frac{(F-F_0)_+}{\hat{F}_0}\right] \frac{B(F)}{B(F_m)} dF}. \tag{4.27}$$

Example 4. If the bonds always renew, i.e. $F_0 = 0$, which might resemble cells in a mesenchymal state, one has the behaviors shown in Fig. 4(a) that is based on the experimental results reported in Refs. 14, 48 and 59. Considering the discussion in Example 3, adding the Darcy’s-like contribution, that is dominant for large velocities, we again have a total interaction force characterized by a cubic-like curve, as the one shown in Fig. 5. In a descriptive way, we might call the increasing branch on the left the mesenchymal-like branch and the one on the right the ameboid-like branch, because the former is characterized by smaller velocities and is adhesion-dominated while the latter is characterized by larger velocities and is related to the difficulties in moving in the network of fibers. So if the stress acting on the cells is too high they might jump to the ameboid-like or Darcy branch and when it decreases again below

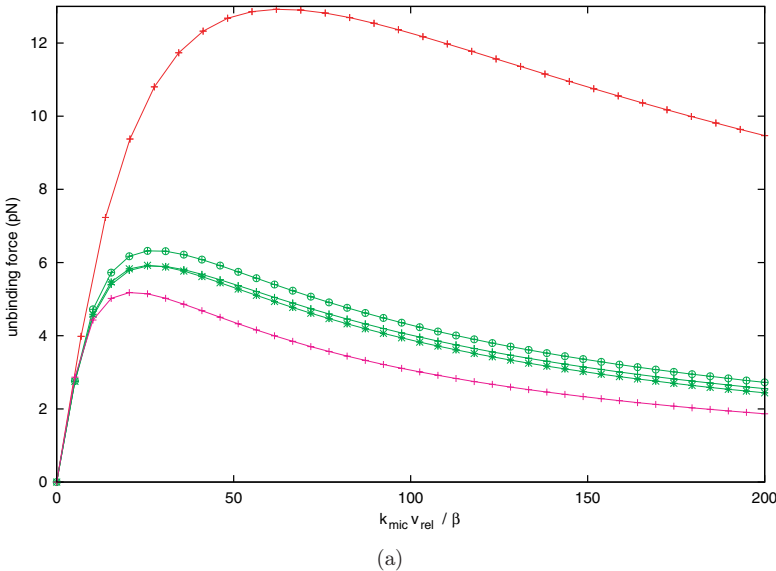


Fig. 4. Macroscopic adhesion laws for the microscopic detachment rates given in Ref. 14 (top), in Ref. 48 (bottom), and in Ref. 59 (the three almost identical in the middle) as given by (4.27). In (a) $F_0 = 0$ and in (b) $F_0 = F_m/2$.

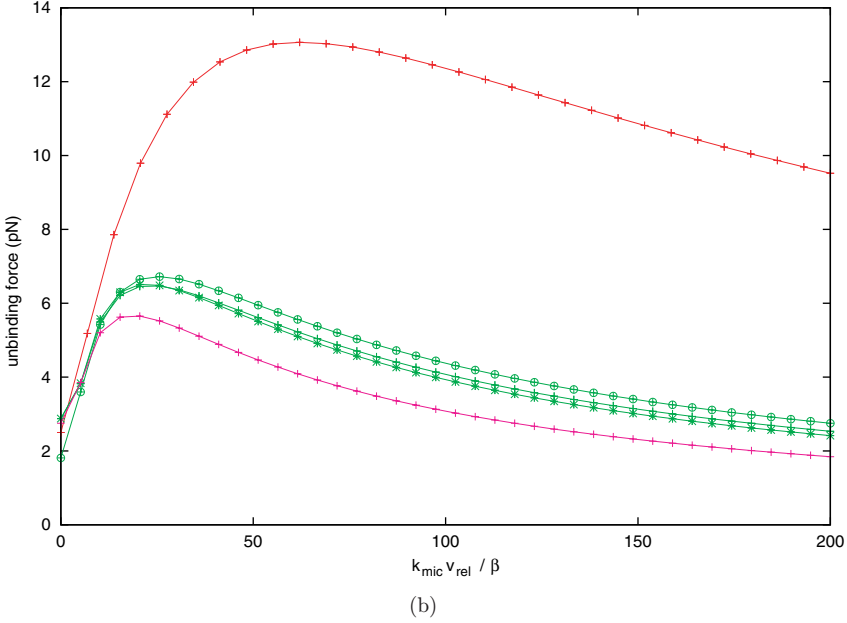


Fig. 4. (Continued)

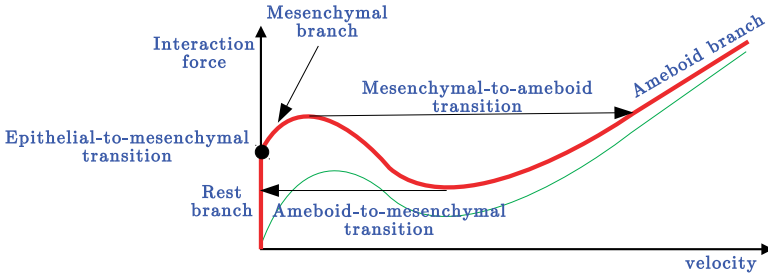


Fig. 5. Sketch of the interaction forces when $F_0 = 0$ (bottom curve) and $F_0 \neq 0$ (upper curves). The right-pointed arrow indicates a transition that resembles the one between mesenchymal and ameboid motion. The left-pointed arrow, the reverse transition. The dot indicates a transition from rest to a mesenchymal-type motion.

the minimum in the graph they will jump to the adhesion-dominated or mesenchymal-like branch. We have then a transition that resembles an ameboid–mesenchymal transition. We, however, need to advise the reader that the above description is a strong simplification, because there are chemical mechanisms that are not considered here, while they are at the basis of the ameboid–mesenchymal transition (see, for instance, Refs. 37, 44, 57 and 58).

Example 5. When $0 \neq F_0 < F_m$, i.e. the threshold for spontaneous renewal is lower than that leading to bond rupture, the behavior of (4.27) is similar to the one

discussed in Example 2, presenting an initial increase from a non-null value that might be described as an epithelial–mesenchymal transition from rest to a slowly moving state. Again we would have a mesenchymal-like (or adhesion-dominated) branch and an ameboid-like (or Darcy-dominated) branch, as in the previous example and shown in Fig. 5. According to whether the local minimum is above or below the threshold value for low velocities, when decreasing the velocity from the ameboid-like branch the cell will go to the mesenchymal-like branch or to the rest branch.

Summarizing, in our opinion, the key features characterizing the link between the properties of the cell–ECM detachment rate and the properties of the macroscopic interaction force are the following.

- The absence of a minimal force needed to trigger cell detachment, e.g. $F_0 = 0$, leads to an interaction force initially proportional to the relative velocity between cells and ECM;
- The presence of a threshold to start breaking the adhesion bonds, e.g. $F_0 \neq 0$, leads to a threshold characterizing the interaction force;
- The existence of a maximum force that can be sustained by the bonds, e.g. F_M , leads for high forces to a regime that is dominated by a contribution proportional to the relative velocity of cell with respect to the ECM similar to Darcy’s law.

As a final remark, as anticipated at the beginning of this section, we notice that if the rate of formation of bonds were simply constant, i.e. in the absence of the integral in the boundary condition (4.1), the above procedure would yield a force blowing up for small velocities because of the absence of the second term in the denominator, for instance of (4.7), and then of the last two terms in (4.14). This biologically corresponds to the fact that if the cell barely moves, bonds always form but never break. So, in the limit an infinite number of bonds form, corresponding to an infinite force. This is of course unphysical and justifies the presence of a saturation term in the boundary condition (4.1).

5. Growth, Cell Reorganization and Stress Tensor

In order to complete the mathematical model, coherently with the arguments used in the previous section and with the results obtained, we now want to transfer the adhesion and detachment mechanisms also to the identification of proper constitutive equations for the stress for the cellular constituent. This requires one to treat cell aggregates as solids and to introduce a threshold value distinguishing the situation in which cells stay attached from the one in which they reorganize, by breaking the bonds and crawling on each other.

As discussed in Refs. 1, 2, 4 and 50, a big theoretical difficulty is encountered in describing tumors and tissues as solid masses because the cells forming them duplicate and die. Even in the absence of growth and death in response to deformation generating unbearable stresses, the ensemble of cells undergoes an internal reorganization, so that the natural configuration always changes.

That is why the concept of an evolving natural configuration introduced by Rajagopal and coworkers can be of help. Actually, the basic idea of this formalism, also present in plasticity theory, started being applied in a biomechanical context to describe growth in Refs. 38, 55 and 60. In the recent past, Humphrey and Rajagopal applied this concept to describe the growth and remodeling of several tissues.^{12,32,33,42,54} Ambrosi and Mollica^{1,2} used a purely elastic one-component model to evaluate residual stress formation in a growing multicellular spheroid. This approach was developed in Refs. 4 and 5 working in a multiphase framework and taking also internal reorganization and ECM deformation into account. This gave rise to an elasto-visco-plastic description for the cell population and an elastic description for the ECM.

In this section we follow Ref. 4 distinguishing in the deformation gradient of the tumor component \mathbf{F}^c the contributions due to pure growth, to cell reorganization and to elastic deformation by a multiplicative decomposition, as shown in Fig. 6.

This splitting is suggested also by the biological observation that the three phenomena occur at different time scales: cell growth and duplication and cell death take many hours up to days, internal reorganization takes several minutes, and typical relaxation times related to viscoelastic phenomena are of the order of seconds. Therefore, it is possible to separate the contributions due to growth, due to cell reorganization and due to deformation (without growth and remodeling) not only to model each of them individually from the theoretical point of view, but also to test each of them from the experimental point of view.

The deformation gradient of the cellular conglomerate $\mathbf{F}^c \in \text{Lin}(\mathbb{T}\mathcal{B}^c, \mathbb{T}\mathcal{B}_t^c)$ is defined as in (2.3) substituting α with c . An imaginary intermediate configuration can be introduced assuming that a point of the body can relieve its state of stress while relaxing the continuity requirement, i.e. the integrity of the body. It then relaxes to a stress-free configuration. The atlas of these pointwise configurations

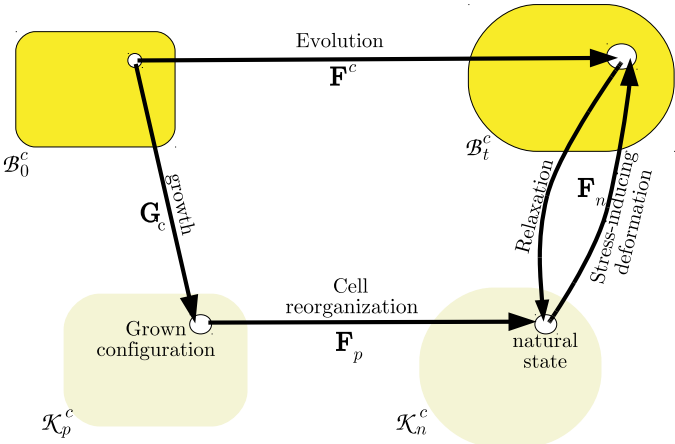


Fig. 6. Multiple natural configuration.

forms what we define the *natural configuration* with respect to \mathcal{B}_t^c and denote by \mathcal{K}_n^c . Referring to Fig. 6, we identify this deformation without growth with the tensor \mathbf{F}_n , which then describes how the body is deforming locally while going from the natural configuration \mathcal{K}_n^c to \mathcal{B}_t^c , in formulas

$$\mathcal{K}_n^c := \mathbf{F}_n^{-1}[\mathbb{T}\mathcal{B}_t^c]. \tag{5.1}$$

The particle in the configuration \mathcal{K}_n^c has possibly undergone growth and plastic deformation. One can then again consider the map from \mathcal{B}_0^c to \mathcal{K}_n^c as composed of two parts: the first one related to growth/death processes (therefore to mass variations in the volume element), the second one due to internal reorganization, which implies rearranging of the adhesion links among the cells, without a change of mass in the volume element. Denoting by \mathcal{K}_p^c the “grown configuration”, i.e. the intermediate configuration of the body between \mathcal{B}_0^c and \mathcal{K}_n^c , we will assume that for any given point the volume ratio in \mathcal{K}_p^c is the same as in the natural configuration \mathcal{K}_n^c and in the original reference configuration \mathcal{B}_0^c , i.e. $\phi_p = \phi_c(t = 0) = \phi_n$. The tensors mapping from a configuration to another are defined as

$$\mathcal{K}_p^c := \mathbf{G}_c[\mathbb{T}\mathcal{B}_0^c], \quad \mathcal{K}_n^c := \mathbf{F}_p[\mathcal{K}_p^c]. \tag{5.2}$$

According to the three-step process outlined above, the deformation gradient is split as

$$\mathbf{F}^c = \mathbf{F}_n \mathbf{F}_p \mathbf{G}_c. \tag{5.3}$$

For sake of simplicity we also take growth to be isotropic $\mathbf{G}_c = g\mathbf{1}$, so that $J_g = \det \mathbf{G}_c = g^3$ and $\mathbf{F}^c = g\mathbf{F}_n \mathbf{F}_p$.

In Ref. 4 it was shown that

$$\frac{\dot{J}_g}{J_g} = 3 \frac{\dot{g}}{g} = \frac{\Gamma_c}{\phi_c}, \tag{5.4}$$

where the dots indicate the time derivative following the cell population. This relation links the evolution of g , i.e. of the first step of the splitting, to the death/growth term Γ_c appearing on the right-hand side of the mass balance equation (3.1) for the cellular constituent.

We now need to determine an evolution equation for the second step of the splitting concerning \mathbf{F}_p . This will be done through an equation determining

$$\mathbf{L}_p = \dot{\mathbf{F}}_p \mathbf{F}_p^{-1}, \quad \text{or} \quad \mathbf{D}_p = \frac{1}{2}(\mathbf{L}_p + \mathbf{L}_p^T). \tag{5.5}$$

Deriving \mathbf{F} with respect to time, we have

$$\dot{\mathbf{F}} = \dot{g}g^{-1}\mathbf{F} + g\dot{\mathbf{F}}_n \mathbf{F}_p + g\mathbf{F}_n \dot{\mathbf{F}}_p = (\dot{g}g^{-1}\mathbf{1} + \mathbf{L}_n + \mathbf{F}_n \mathbf{L}_p \mathbf{F}_n^{-1})\mathbf{F}, \tag{5.6}$$

where $\mathbf{L}_n = \dot{\mathbf{F}}_n \mathbf{F}_n^{-1}$ that, through the usual definition of $\mathbf{L} = \dot{\mathbf{F}}\mathbf{F}^{-1}$ can be rewritten as

$$\mathbf{L}_n = \mathbf{L} - \dot{g}g^{-1}\mathbf{1} - \mathbf{F}_n \mathbf{L}_p \mathbf{F}_n^{-1}. \tag{5.7}$$

On the other hand, deriving the left Cauchy–Green tensor related to the recoverable part of the deformation

$$\mathbf{B}_n = \mathbf{F}_n \mathbf{F}_n^T, \tag{5.8}$$

with respect to time, one has

$$\begin{aligned} \dot{\mathbf{B}}_n &= \mathbf{L}_n \mathbf{B}_n + \mathbf{B}_n \mathbf{L}_n^T \\ &= \mathbf{L} \mathbf{B}_n + \mathbf{B}_n \mathbf{L}^T - 2\dot{g}g^{-1} \mathbf{B}_n - 2\mathbf{F}_n \mathbf{D}_p \mathbf{F}_n^T. \end{aligned} \tag{5.9}$$

Finally, if the definition of upper convected Maxwell derivative,

$$\frac{\mathcal{D}\mathbf{M}}{\mathcal{D}t} = \dot{\mathbf{M}} - \mathbf{L}\mathbf{M} - \mathbf{M}\mathbf{L}^T, \tag{5.10}$$

is introduced

$$\frac{\mathcal{D}\mathbf{B}_n}{\mathcal{D}t} = -2\dot{g}g^{-1} \mathbf{B}_n - 2\mathbf{F}_n \mathbf{D}_p \mathbf{F}_n^T. \tag{5.11}$$

We want now to include elasto-visco-plastic effects in the mechanics of cell aggregates. We do that on the basis of the following observations:

- (1) when and where the cell populations is subject to a moderate amount of stress, then the body behaves elastically;
- (2) when and where the stress overcomes a threshold yield stress, then the body undergoes visco-plastic deformations.

Given the resistance of a single bond, the threshold of the onset of plastic deformations is proportional to the area of the cell membranes in contact, which depends on the number of cells per unit volume. We call yield stress this threshold value $\tau(\phi)$ and compare it with a frame invariant measure f of the stress of the cellular constituent $\phi_c \mathbf{T}_c$.

On this basis, the following elastic-type constitutive equation can be suggested in the elastic regime

$$\mathbf{T}_c = \hat{\mathbf{T}}_c(\mathbf{B}_n), \quad \text{if } f(\phi_c \mathbf{T}_c) \leq \tau(\phi), \tag{5.12}$$

where, following Ref. 13, we take as a measure of the stress the maximum shear stress magnitude

$$f(\phi_c \mathbf{T}_c) = \max_{|\mathbf{n}|=1} |\phi_c [\mathbf{T}_c \mathbf{n} - (\mathbf{n} \cdot \mathbf{T}_c \mathbf{n}) \mathbf{n}]|. \tag{5.13}$$

It can be proved (see, for instance, Ref. 43) that f is given by half of the difference between the maximum and the minimum eigenvalue of $\phi_c \mathbf{T}_c$.

Following Ref. 4, above the yield stress the tension in excess originates from cell unbinding at the microscopic scale and then cell rearrangement at the macroscopic scale. Such a pictorial description is put into formal terms by the following

constitutive equation that is a modified and corrected version of the one proposed in Ref. 4:

$$\left[1 - \left(\frac{\tau(\phi_c)}{f(\phi_c \mathbf{T}'_c)}\right)^\alpha\right] (\phi_c \mathbf{F}_n^T \mathbf{T}'_c \mathbf{F}_n^{-T}) = 2\eta(\phi_c) \mathbf{L}_p \quad \text{if } f(\phi_c \mathbf{T}'_c) > \tau(\phi_c), \quad (5.14)$$

where $\mathbf{T}'_c = \mathbf{T}_c - \frac{1}{3}(\text{tr} \mathbf{T}_c) \mathbf{1}$ operates on the current configuration and for compatibility we mapped \mathbf{D}_p into the same configuration using \mathbf{F}_n . We can merge the above equation to the condition that there is no evolution for shear stresses smaller than the yield stress by writing

$$\mathbf{F}_n^{-T} \mathbf{L}_p \mathbf{F}_n^T = \frac{1}{2\tilde{\eta}} \left[1 - \frac{1}{\tilde{f}(\mathbf{T}'_c)}\right]_+ \mathbf{T}'_c, \quad (5.15)$$

where $[\cdot]_+$ stands for the positive part of the argument, $\tilde{\eta} = \eta(\phi_c)/\phi_c$, and $\tilde{f}(\mathbf{T}'_c) = [f(\phi_c \mathbf{T}'_c)/\tau(\phi_c)]^\alpha$.

Following Ref. 24, it is worth stating how the quantities introduced above transform under a change of frame. Denoting with a star (*) the value of a field after a Euclidean change of frame, one has

$$\begin{aligned} \mathbf{F}_n^* &= \mathbf{Q} \mathbf{F}_n, \\ \mathbf{G}_c^* &= \mathbf{G}_c, \\ \mathbf{F}_p^* &= \mathbf{F}_p, \end{aligned}$$

for all \mathbf{Q} orthogonal tensors.

Thanks to the previous relations

$$(\mathbf{F}_n^{-T} \mathbf{L}_p \mathbf{F}_n^T)^* = \mathbf{Q} \mathbf{F}_n^{-T} \mathbf{L}_p \mathbf{F}_n^T \mathbf{Q},$$

being \mathbf{T}_c objective, one has the objectivity of (5.15).

If we take the following elastic-type constitutive equation

$$\mathbf{T}'_c = \mu \left(\mathbf{B}_n - \frac{1}{3}(\text{tr} \mathbf{B}_n) \mathbf{1} \right), \quad (5.16)$$

then, \mathbf{F}_p evolves according to

$$\dot{\mathbf{F}}_p = \frac{g^{-1}}{\lambda} \left[1 - \frac{1}{\mu \tilde{f}(\mathbf{B}_n - \frac{1}{3}(\text{tr} \mathbf{B}_n) \mathbf{1})} \right]_- + \left(\mathbf{C}_n - \frac{1}{3}(\text{tr} \mathbf{C}_n) \mathbf{1} \right) \mathbf{F}_p, \quad (5.17)$$

where $\lambda = \frac{\tilde{\eta}}{\mu}$ is called the *cell reorganization time* and $\mathbf{C}_n = \mathbf{F}_n^T \mathbf{F}_n$.

Equation (5.17) can be explained phenomenologically in the following way: assuming for a moment that there is no growth, if the body undergoes a deformation corresponding to a measure of the stress below the yield stress, then \mathbf{F}_p does not change, i.e. the intermediate configuration does not evolve and all the energy is elastically stored. If the measure of tension f takes a value larger than the yield stress, then the reference configuration changes to release the stress in excess, until the yield

surface defined by f is reached again. The ratio $\lambda = \frac{\bar{t}}{\mu}$ gives an indication of the characteristic time needed to relax the internal stress through the reorganization of cells and to reach the yield surface.

We want now to eliminate \mathbf{D}_p from the constitutive equation for the stress. The first step to do that consists in deriving (5.16) to write

$$\begin{aligned} \dot{\mathbf{T}}'_c = \mu & \left[\mathbf{L}\mathbf{B}_n + \mathbf{B}_n\mathbf{L}^T - 2\dot{g}g^{-1}\mathbf{B}_n - 2\mathbf{F}_n\mathbf{D}_p\mathbf{F}_n^T \right. \\ & \left. - \frac{1}{3}\text{tr}(\mathbf{L}\mathbf{B}_n + \mathbf{B}_n\mathbf{L}^T - 2\dot{g}g^{-1}\mathbf{B}_n - 2\mathbf{F}_n\mathbf{D}_p\mathbf{F}_n^T)\mathbf{1} \right]. \end{aligned}$$

We can then use (5.15) to get

$$\begin{aligned} \dot{\mathbf{T}}'_c + \frac{\mu}{\tilde{\eta}} & \left[1 - \frac{1}{\tilde{f}(\mathbf{T}'_c)} \right]_+ \left(\mathbf{T}'_c\mathbf{B}_n + \mathbf{B}_n\mathbf{T}'_c - \frac{1}{3}\text{tr}(\mathbf{T}'_c\mathbf{B}_n + \mathbf{B}_n\mathbf{T}'_c)\mathbf{1} \right) \\ & = \mu[\mathbf{L}\mathbf{B}_n + \mathbf{B}_n\mathbf{L}^T - 2\dot{g}g^{-1}\mathbf{B}_n - \frac{1}{3}\text{tr}(\mathbf{L}\mathbf{B}_n + \mathbf{B}_n\mathbf{L}^T - 2\dot{g}g^{-1}\mathbf{B}_n)\mathbf{1}], \end{aligned}$$

which can be written in terms of upper convective derivative as

$$\begin{aligned} \frac{D\mathbf{T}'_c}{Dt} + \frac{1}{\lambda} & \left[1 - \frac{1}{\tilde{f}(\mathbf{T}'_c)} \right]_+ \left(\mathbf{T}'_c\mathbf{B}_n + \mathbf{B}_n\mathbf{T}'_c - \frac{2}{3}\text{tr}(\mathbf{T}'_c\mathbf{B}_n)\mathbf{1} \right) \\ & = \frac{2}{3}\mu[\text{tr}(\mathbf{B}_n)\mathbf{D} - \text{tr}(\mathbf{B}_n\mathbf{D})\mathbf{1} - \dot{g}g^{-1}(3\mathbf{B}_n - (\text{tr}\mathbf{B}_n)\mathbf{1})]. \end{aligned} \tag{5.18}$$

Note that the Maxwell derivative of an objective tensor is itself objective.

The above constitutive equation can be simplified considerably assuming that the deformations from the natural configuration are small throughout the evolution of the system and that $g = 1$, corresponding to no growth. The small deformation assumption applies depending on the value of the yield stress: it has to be small enough so that the condition $|\mathbf{B}_n \cdot \mathbf{1} - 3| \ll 1$ is always satisfied during the motion. The experiments by Jordan *et al.*³⁵ give an indication of the order of magnitude of the yield stress, which depends on the volume ratio and is below 1 Pa (for $\phi_c = 0.6$, the maximum volume ratio tested). The advantage of this hypothesis is that for small elastic strain one can use linear elasticity. For larger stresses, the natural configuration evolves. In the limit of small deformations,

$$\mathbf{L}\mathbf{B}_n + \mathbf{B}_n\mathbf{L}^T \approx 2\mathbf{D}, \quad \text{and} \quad \mathbf{T}'_c\mathbf{B}_n \approx \mathbf{B}_n\mathbf{T}'_c \approx \mathbf{T}'_c, \tag{5.19}$$

and therefore (5.18) simplifies to

$$\dot{\mathbf{T}}'_c + \frac{1}{\lambda} \left[1 - \frac{1}{\tilde{f}(\mathbf{T}'_c)} \right]_+ \mathbf{T}'_c = 2\mu \left(\mathbf{D} - \frac{1}{3}(\text{tr}\mathbf{D})\mathbf{1} \right), \tag{5.20}$$

where the trace of \mathbf{D} is related to the growth term through the mass balance equation.

We observe that in (5.20), the term containing the yield stress plays the role of a stress relaxation term that switches on as soon as the stress is above the yield value.

Otherwise, for $\tilde{f}(\mathbf{T}'_c) < 1$, (5.20) can be integrated to give back an elastic-like constitutive equation.

The limit λ much larger than the characteristic time of the process of interest, in principle would lead to the models used for instance in Refs. 6, 8, 9 and 36. However, in this case the procedure is incompatible with the small deformation assumption because the stress relaxes very slowly and so large stresses and deformation can build up.

On the other hand, rewriting (5.20) as

$$\lambda \dot{\mathbf{T}}'_c + \left[1 - \frac{1}{\tilde{f}(\mathbf{T}'_c)} \right]_+ \mathbf{T}'_c = 2\eta \left(\mathbf{D} - \frac{1}{3} (\text{tr} \mathbf{D}) \mathbf{1} \right), \tag{5.21}$$

makes it easy to realize that for processes with characteristic times larger than λ and stresses much larger than τ (i.e. $\tilde{f} \gg 1$) the model behaves like the viscous models used in Refs. 27–29.

6. Results

As a preliminary example, we consider a tumor growing in a region delimited by a thick extracellular membrane that, however, presents a hole in the middle. Another region with a dense ECM is in the top-left region. We assume that the ECM is rigid, non-homogeneous with a given $\phi_m(\mathbf{x})$ filling 50% of the space within the membrane and 20% of the space elsewhere. We also assume that the tumor has all the nutrients necessary to grow but that cells are inhibited by contact when the stress acting on them is too high, with a difference in sensitivity between tumor and host cells as in Ref. 22. Specifically, compared to normal cells, tumor cells stop duplication (after stress relaxation) at $\phi_c = 0.6$ rather than at $\phi_c = 0.5$. The region $\Omega_T(t)$ occupied by the tumor is identified in the following equation by the function $\chi_{\Omega_T}(\mathbf{x}, t)$. Due to the presence of a moving interface dividing the two domains we used a level-set method.^{22,23,39,45,40,66}

With the idea of focusing on the cell-ECM interaction we start with the simplest model that contains the main adhesion features described in Sec. 4 and related to the experiments through the relation (4.25). For this reason we consider negligible the contribution due to \mathbf{T}'_c and assume that the stress is simply given by the isotropic part $\Sigma(\phi_c) = E(\phi_c - \phi_0)/(1 - \phi_c)$, so that the model can be written as

$$\begin{cases} \frac{\partial \phi_c}{\partial t} + \nabla \cdot (\phi_c \mathbf{v}_c) = [\gamma H(\phi_0 + \Delta \chi_{\Omega_T}(\mathbf{x}, t) - \phi_c) - \delta] \phi_c, \\ -\nabla \Sigma(\phi_c) = \left[N_{\max}(\phi_m) \frac{\sigma^2 + m_b^2}{2(m_b + \frac{k_{\text{mic}} v_c}{\beta}) v_c} + M(\phi_m) \right] \mathbf{v}_c, \end{cases} \tag{6.1}$$

where γ is the growth rate, δ is the death rate, H is the Heaviside function, so that growth activates when the cell volume ratio is below ϕ_0 for normal cells and $\phi_0 + \Delta$ for tumor cells.

As put in evidence in the equations above, both M and N_{\max} depend on the volume ratio occupied by the ECM. Since in the example we want to focus on, the

environment is strongly heterogeneous we need to specify this dependence. The former coefficient is related to the fact that, roughly speaking, less space is available for the cells to move. For M we then take Kozeny–Carman relationship $M = M_0(\phi_m^2(1 - \hat{\phi}_m)^3/\hat{\phi}_m^2(1 - \phi_m)^3)$ where M_0 is the resistivity at the assumed physiological volume ratio of ECM $\hat{\phi}_m = 0.2$. The latter is mainly related to the fact that the contact area between cell membranes and ECM fibers increases with the density of fibers. We take this relationship to be linear $N_{\max} = N_0\phi_m$, though it might be more complicated than that.

It is convenient to rewrite the system in dimensionless variables, introducing the typical time scale $T = \frac{1}{\gamma}$ and choosing the typical length scale $L = \sqrt{\frac{E}{M_0\gamma}}$

$$\begin{cases} \frac{\partial \phi_c}{\partial t} + \tilde{\nabla} \cdot (\phi_c \mathbf{v}_c) = [H(\phi_0 + \Delta\chi_{\Omega_T} - \phi_c) - \tilde{\delta}]\phi_c, \\ -\frac{(1 - \phi_0)}{(1 - \phi_c)^2} \tilde{\nabla} \phi_c = \left[\tilde{N}_0 \frac{\phi_m}{(1 + \tilde{k}\tilde{v}_c)\tilde{v}_c} + \frac{\phi_m^2(1 - \hat{\phi}_m)^3}{\hat{\phi}_m^2(1 - \phi_m)^3} \right] \tilde{\mathbf{v}}_c, \end{cases} \tag{6.2}$$

where tildes denote dimensionless variables and

$$\tilde{\delta} = \frac{\delta}{\gamma}, \quad \tilde{N}_0 = \frac{N_0 m_b}{2\sqrt{EM_0\gamma}} \left(1 + \frac{\sigma^2}{m_b^2} \right), \quad \tilde{k} = \frac{k}{\beta m_b} \sqrt{\frac{E\gamma}{M_0}}$$

We impose no flux boundary conditions on the x -axis and on the y -axis, till the membrane. On the remaining part of the y -axis and on the other two sides of the rectangular domain $[0, 16] \times [0, 10]$ the stress-free volume ratio $\phi_c = \phi_0 = 0.5$ is imposed. Initially, the tumor is put in a small region near the bottom-left corner with a volume ratio $\phi_c = \phi_0 = 0.5$ as the host tissue. The simulation shown in Fig. 7 is performed setting $\tilde{\delta} = 0.2$, $\tilde{N}_0 = 1.75$, and $\tilde{k} = 0.5$.

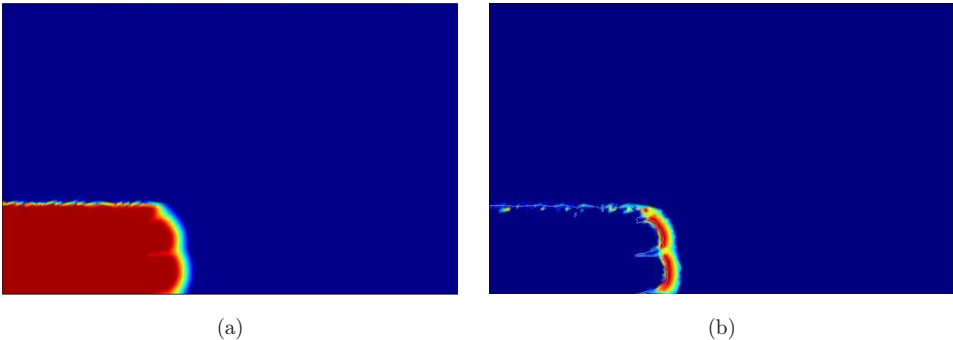


Fig. 7. Tumor growing in presence of an ECM membrane. (a) Volume ratio at $t = 50$ days. (b) Interaction force at $t = 50$ days. (c) Volume ratio at $t = 100$ days. (d) Interaction force at $t = 100$ days. In (a)–(d) the line is the tumor border. (e) Closeup of a region near the tumor border at $t = 125$ days. The line delimitates the region with relative motion between cells and ECM.

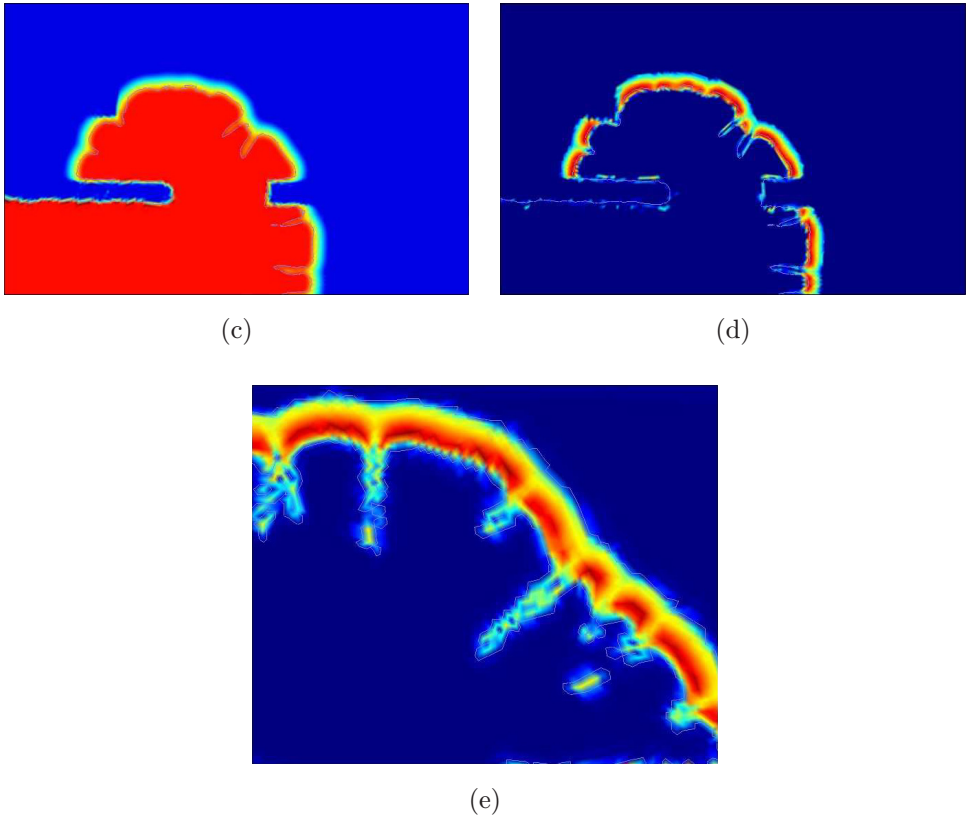


Fig. 7. (Continued)

In Figs. 7(a) and 7(c) the volume ratio of the tumor is higher than the surrounding tissue because they are less sensitive to contact inhibition. The volume ratios in the bulks of the tissue and of the tumor are nearly constant. It changes near the border of the tumor where the surrounding tissue is compressed by the growing mass. The front seems to present a sort of instability as that characterizing some of the simulations in Ref. 41. When the tumor growing from the bottom-left corner reaches the membrane, it is hard for the cells to cross it because of the increased number of the adhesion bonds (N_{\max} is taken to be proportional to $\phi_m(\mathbf{x})$) and the decreased permeability (satisfying a Kozeny–Karman relationship). It is then easier for the tumor to grow toward the right (see Fig. 7(a)) with the central region that become contact inhibited with an interaction force below that necessary to trigger motility. In fact, as shown in Fig. 7(b), the region with cells that are moving relative to the ECM is close to the border of the tumor. This is also the region where cells duplicate the most. When the hole is reached the tumor moves across it surrounding the membrane also on its other side (see Figs. 7(c) and 7(d)). Finally, in Fig. 7(e) we plot a blowup of the interfacial force. The contour line corresponds to the threshold triggering motion, so that the

cells inside this region detach from the ECM. Looking carefully one can notice that outside this region there are small zones with non-vanishing interfacial forces, but not strong enough to trigger detachment.

7. Discussion and Possible Developments

In this paper we have shown how the information obtained performing experiments at the sub-cellular scale on the detachment forces of single adhesion bonds can be upscaled and be used in a macroscopic model. For instance, an easy formula (4.14) linking the adhesive interaction force present in the multiphase model with the mean and standard deviation of the bond-breaking probability, the microscopic elastic constant, the bond renewal rate, and the maximum number density of adhesive sites is found. An unexpected by-product of the study of cell–ECM interaction is the deduction of some laws that qualitatively lead to behaviors like the epithelial–mesenchymal transition and the mesenchymal–ameboid transition. We are well aware that the comparison can only be qualitative because our description is purely mechanical, neglecting all the chemical phenomena triggering such transitions (see, for instance, Refs. 37, 44, 57 and 58) and that, for instance, from the viewpoint presented here can at least change the parameters. However, in our opinion such constitutive laws for the interaction force present in the multiphase model is by itself very interesting also from the mathematical point of view. In fact, they are likely to give rise to bistable behaviors and to the presence of hysteresis cycles. However, such characteristics were here only argued and not proved mathematically. Also from the numerical point of view, the use of such non-monotonic laws is not trivial and need some care. In a future work we will describe how to do that applying the model to the behavior of multicellular aggregates under compression and shear condition.

Other developments can be obtained taking into account several phenomena not considered here and that can influence cell–cell adhesion and cell–ECM adhesion. For instance, it is known that in a tumor mass there are several clones characterized by different adhesive behaviors and motilities, that hypoxia can induce changes in adhesion and trigger cell motility, and there are actually several chemical factors influencing the transition of cells to a mesenchymal state.

Coming to the deduction of the constitutive equation for the stress, coherently with what was done for the interfacial forces, we explained how the same attachment/detachment processes may generate internal cell reorganization when and where the stress is larger than the value that can be sustained by the adhesion bonds. This was done using the concept of evolving natural configurations that might be also very useful to describe ECM remodeling. This phenomenon involves on one side the production of matrix degrading enzymes breaking the possibly stretched ECM fibers and on the other side the concomitant reconstruction of ECM mainly by fibroblasts depositing unstretched fibers. So, also in this case the material and the corresponding natural configurations are continuously evolving.

Acknowledgments

The authors thank F. Pellerey, C. Schmeiser, and A. Tosin for fruitful discussions. This work was partially supported by the Italian Ministry for University and Research, through a PRIN project on “Modelli matematici dell’interazione meccanica di cellule singole e di aggregati cellulari con l’ambiente circostante”.

References

1. D. Ambrosi and F. Mollica, On the mechanics of a growing tumor, *Int. J. Engrg. Sci.* **40** (2002) 1297–1316.
2. D. Ambrosi and F. Mollica, The role of stress in the growth of a multicell spheroid, *J. Math. Biol.* **48** (2004) 477–499.
3. D. Ambrosi and L. Preziosi, On the closure of mass balance models for tumor growth, *Math. Models Methods Appl. Sci.* **12** (2002) 737–754.
4. D. Ambrosi and L. Preziosi, Cell adhesion mechanisms and stress relaxation in the mechanics of tumours, *Biomech. Model. Mechanobiol.* **8** (2009) 397–413.
5. D. Ambrosi, L. Preziosi and G. Vitale, The insight of mixture theory for growth and remodeling, *Z. Angew. Math. Phys.* **61** (2010) 177–191.
6. R. P. Araujo and D. L. S. McElwain, A linear-elastic model of anisotropic tumour growth, *Eur. J. Appl. Math.* **15** (2004) 365–384.
7. R. P. Araujo and D. L. S. McElwain, A history of the study of solid tumour growth: The contribution of mathematical modeling, *Bull. Math. Biol.* **66** (2004) 1039–1091.
8. R. P. Araujo and D. L. S. McElwain, A mixture theory for the genesis of residual stresses in growing tissues, I: A general formulation, *SIAM J. Appl. Math.* **65** (2005) 1261–1284.
9. R. P. Araujo and D. L. S. McElwain, A mixture theory for the genesis of residual stresses in growing tissues, II: Solutions to the biphasic equations for a multicell spheroid, *SIAM J. Appl. Math.* **65** (2005) 1285–1299.
10. N. J. Armstrong, K. J. Painter and J. A. Sherratt, A continuum approach to modelling cell–cell adhesion, *J. Theor. Biol.* **243** (2006) 98–113.
11. N. J. Armstrong, K. J. Painter and J. A. Sherratt, Adding adhesion to the cell cycle model for somite formation, *Bull. Math. Biol.* **71** (2009) 1–24.
12. S. Baek, K. R. Rajagopal and J. D. Humphrey, A theoretical model of enlarging intracranial fusiform aneurysms, *J. Biomech. Engrg.* **128** (2006) 142–149.
13. I. V. Basov and V. V. Shelukhin, Generalized solutions to the equations of compressible Bingham flows, *Z. Angew. Math. Mech.* **79** (1999) 185–192.
14. W. Baumgartner, P. Hinterdorfer, W. Ness, A. Raab, D. Vestweber and H. D. D. Schindler, Cadherin interaction probed by atomic force microscopy, *Proc. Natl. Acad. Sci. USA* **97** (2000) 4005–4010.
15. N. Bellomo, *Modeling Complex Living Systems — Kinetic Theory and Stochastic Game Approach* (Birkhäuser, 2008).
16. N. Bellomo, N. K. Li and P. K. Maini, On the foundations of cancer modelling: Selected topics, speculations and perspectives, *Math. Models Methods Appl. Sci.* **18** (2008) 593–646.
17. R. M. Bowen, Theory of mixtures, in *Continuum Physics*, ed. A. C. Eringen (Academic Press, New York, 1976).
18. R. M. Bowen, Incompressible porous media models by the use of the theory of mixtures, *Int. J. Engrg. Sci.* **18** (1980) 1129–1148.

19. R. M. Bowen, Compressible porous media models by the use of the theory of mixtures, *Int. J. Engrg. Sci.* **20** (1982) 697–735.
20. H. Byrne and L. Preziosi, Modeling solid tumor growth using the theory of mixtures, *Math. Med. Biol.* **20** (2004) 341–360.
21. E. Canetta, A. Duperray, A. Leyrat and C. Verdier, Measuring cell viscoelastic properties using a force-spectrometer: Influence of the protein–cytoplasm interactions, *Biorheology* **42** (2005) 298–303.
22. M. Chaplain, L. Graziano and L. Preziosi, Mathematical modelling of the loss of tissue compression responsiveness and its role in solid tumour development, *Math. Med. Biol.* **23** (2005) 197–229.
23. V. Cristini, X. Li, J. Lowengrub and S. M. Wise, Nonlinear simulations of solid tumor growth using a mixture model: Invasion and branching, *J. Math. Biol.* **58** (2009) 723–763.
24. A. DiCarlo and S. Quiligotti, Growth and balance, *Mech. Res. Commun.* **29** (2002) 449–456.
25. G. Forgacs, R. Foty, Y. Shafrir and M. Steinberg, Viscoelastic properties of living embryonic tissues: A quantitative study, *Biophys. J.* **74** (1998) 2227–2234.
26. R. A. Foty, G. Forgacs, S. Pfleger and M. Steinberg, Surface tensions of embryonic tissues predict their mutual envelopment behavior, *Development* **122** (1996) 1611–1620.
27. S. Franks, H. Byrne, J. King, J. Underwood and C. Lewis, Modelling the early growth of ductal carcinoma *in situ* of the breast, *J. Math. Biol.* **47** (2003) 424–452.
28. S. Franks, H. Byrne, H. Mudhar, J. Underwood and C. Lewis, Mathematical modelling of comedo ductal carcinoma *in situ* of the breast, *Math. Med. Biol.* **20** (2003) 277–308.
29. S. Franks and J. King, Interactions between a uniformly proliferating tumor and its surrounding uniform material properties, *Math. Med. Biol.* **20** (2003) 47–89.
30. L. Graziano and L. Preziosi, Mechanics in tumour growth, in *Modeling of Biological Materials*, eds. K. Rajagopal, F. Mollica and L. Preziosi (Birkhäuser, 2007), pp. 267–328.
31. T. Hillen, K. Painter and C. Schmeiser, Global existence for chemotaxis with finite sampling radius, *Discrete Contin. Dyn. Syst.* **7** (2007) 125–144.
32. J. Humphrey and K. Rajagopal, A constrained mixture model for growth and remodeling of soft tissues, *Math. Models Methods Appl. Sci.* **22** (2002) 407–430.
33. J. Humphrey and K. Rajagopal, A constrained mixture model for arterial adaptations to a sustained step change in blood flow, *Biomech. Model. Mechanobiol.* **2** (2003) 109–126.
34. M. Iannelli, M. Martcheva and F. A. Milner, Gender-structured population modeling — Mathematical methods, numerics, and simulations, *SIAM Frontiers Appl. Math.* (2005).
35. A. Jordan, A. Duperray and C. Verdier, Fractal approach to the rheology of concentrated cell suspensions, *Phys. Rev. E* **77** (2008) 011911.
36. A. F. Jones, H. M. Byrne, J. S. Gibson and J. W. Dold, A mathematical model of the stress induced during solid tumour growth, *J. Math. Biol.* **40** (2000) 473–499.
37. J. Jou and A. M. Diehl, Epithelial-mesenchymal transitions and hepatocarcinogenesis, *J. Clin. Invest.* **120** (2010) 1031–1034.
38. S. M. Klisch and A. Hoger, Volumetric growth of thermoelastic materials and mixtures, *Math. Mech. Solids* **8** (2003) 377–402.
39. J. S. Lowengrub, H. B. Frieboes, F. Jin, Y. L. Chuang, X. Li, P. Macklin, S. M. Wise and V. Cristini, Nonlinear modelling of cancer: Bridging the gap between cells and tumours, *Nonlinearity* **23** (2010) R1–R91.
40. J. Lowengrub, S. M. Wise, H. B. Frieboes and V. Cristini, Three-dimensional multispecies nonlinear tumor growth, I: Model and numerical method, *J. Theor. Biol.* **253** (2008) 524–543.
41. P. Macklin and J. Lowengrub, Nonlinear simulation of the effect of the microenvironment on tumor growth, *J. Theor. Biol.* **245** (2007) 677–704.

42. W. A. Malik, S. C. Prasad, K. R. Rajagopal and L. Preziosi, On the modeling of the viscoelastic response of embryonic tissues, *Math. Mech. Solids* **13** (2008) 81–91.
43. L. E. Malvern, *Introduction of the Mechanics of a Continuous Medium* (Prentice-Hall, 1969).
44. M. Novotny, J. Brabek, K. Pankova and D. Rosel, The molecular mechanisms of transition between mesenchymal and amoeboid invasiveness in tumor cells, *Cell. Mol. Life Sci.* **67** (2010) 63–71.
45. J. T. Oden, A. Hawkins and S. Proudhomme, General diffuse-interface theories and an approach to predictive tumor growth modeling, *Math. Models Methods Appl. Sci.* **20** (2010) 477–517.
46. D. Ölz and C. Schmeiser, How do cells move? Mathematical modelling of cytoskeleton dynamics and cell migration, in *Cell Mechanics: From Single Scale-Based Model to Multiscale Modeling*, eds. L. Preziosi A. Chauviere and C. Verdier (Chapman and Hall/CRC Press, 2010).
47. D. Ölz, C. Schmeiser and V. Small, Modelling of the actin-cytoskeleton in symmetric lamellipodial fragments, *Cell Adhesion Migration* **2** (2008) 117–126.
48. P. Panorchan, M. S. Thompson, K. J. Davis, Y. Tseng, K. Konstantopoulos and D. Wirtz, Single-molecule analysis of cadherin-mediated cell–cell adhesion, *J. Cell Sci.* **119** (2006) 66–74.
49. J. J. Pop and R. M. Bowen, A theory of mixtures with a long range spatial interaction, *Acta Mech.* **29** (1978) 21–34.
50. L. Preziosi, D. Ambrosi and C. Verdier, An elasto-visco-plastic model of cell aggregates, *J. Theor. Biol.* **262** (2010) 35–47.
51. L. Preziosi and A. Farina, On Darcy’s law for growing porous media, *Int. J. Nonlinear Mech.* **37** (2001) 485–491.
52. L. Preziosi and A. Tosin, Multiphase and multiscale trends in cancer modelling, *Math. Model. Natl. Phenom.* **4** (2009) 1–11.
53. L. Preziosi and A. Tosin, Multiphase modeling of tumor growth and extracellular matrix interaction: Mathematical tools and applications, *J. Math. Biol.* **58** (2009) 625–656.
54. I. Rao, J. Humphrey and K. Rajagopal, Biological growth and remodeling: A uniaxial example with possible application to tendons and ligaments, *Comp. Mod. Engrg. Sci.* **4** (2003) 439–495.
55. E. K. Rodriguez, A. Hoger and A. McCulloch, Stress-dependent finite growth in soft elastic tissues, *J. Biomechanics* **27** (1994) 455–467.
56. C. Schmeiser and D. Ölz, Derivation of a model for symmetric lamellipodia with instantaneous cross-link turnover, *Arch. Rational Mech. Anal.* **198** (2010) 963–980.
57. M. Scianna, R. Merks, L. Preziosi and E. Medico, Individual cell-based models of cell scatter of aro and mlp-29 cells in response to hepatocyte growth factor, *J. Theor. Biol.* **260** (2009) 151–160.
58. M. Scianna, L. Munaron and L. Preziosi, A multiscale hybrid approach for vasculogenesis and related potential blocking therapies, submitted to *Prog. Biophys. Mol. Biol.*, DOI: 10.1016/p.biomolbio.2011.01.004.
59. M. Sun, J. Graham, B. Hegedus, F. Marga, Y. Zhang, G. Forgacs and M. Grandbois, Multiple membrane tethers probed by atomic force microscopy, *Biophys. J.* **89** (2005) 4320–4329.
60. L. A. Taber and J. D. Humphrey, Stress modulated growth, residual stress and vascular heterogeneity, *ASME J. Biomech. Engrg.* **123** (2001) 528–535.
61. P. Tracqui, Biophysical models of tumour growth, *Rep. Prog. Phys.* **72** (2009) 056701.
62. D. Valdembri, P. T. Caswell, K. I. Anderson, J. P. Schwartz, E. Astanina, F. Caccavari, J. C. Norman, M. J. Humphries, F. Bussolino and G. Serini, Neuropilin-1/gipc1 signaling

- regulates $\alpha 5 \beta 1$ integrin traffic and function in endothelial cells, *PLoS Biol.* **7** (2009), DOI:10.1371/journal.pbio.1000025.
63. C. Verdier, J. Etienen, A. Duperray and L. Preziosi, Review: Rheological properties of biological materials, *C. R. Acad. Sci. Phys.* **10** (2009) 790–811.
 64. K. Wilmanski, Lagrangean model of a two phases porous material, *J. Non-Equilib. Thermodyn.* **20** (1995) 50–77.
 65. B. Winters, S. Shepard and R. Foty, Biophysical measurement of brain tumor cohesion, *Int. J. Cancer* **114** (2005) 371–379.
 66. S. M. Wise, J. Lowengrub, H. B. Frieboes, F. Jin, Y. L. Chuang and V. Cristini, Three-dimensional multispecies nonlinear tumor growth, II: Tumor invasion and angiogenesis, *J. Theor. Biol.* **264** (2010) 1254–1278.
 67. L. Yuan, M. J. Fairchild, A. D. Perkins and G. Tanentzapf, Analysis of integrin turnover in fly myotendinous junctions, *J. Cell Sci.* **123** (2010) 939–946.